Evaluation of cell-based and surrogate SARS-CoV-2 neutralization assays

Running title (54 characters): Evaluation of SARS-CoV-2 neutralizing antibody assays

Anton M. Sholukh[1*#], Andrew Fiore-Gartland[1*], Emily S. Ford[1,3], Maurine D. Miner[1], Yixuan J. Hou[5], Longping V. Tse[5], Hannah Kaiser[7], Haiying Zhu[4], Joyce Lu[4], Bhanupriya Madarampalli[4], Arnold Park[7], Florian A. Lempp[7], Russell St. Germain[1], Emily L. Bossard[1], Jia Jin Kee[1], Kurt Diem[4], Andrew B. Stuart[1], Peter B. Rupert[2], Chance Brock[2], Matthew Buerger[2], Margaret K. Doll[10], April Kaur Randhawa[1], Leonidas Stamatatos[1], Roland K. Strong[1,2], Colleen McLaughlin[10], Meei-Li Huang[4], Keith R. Jerome[1,4], Ralph S. Baric[5,6], David Montefiori[8,9], and Lawrence Corey[1,3,4#]

[1]Vaccine and Infectious Diseases Division, Fred Hutch Cancer Research Center, Seattle WA
[2]Basic Sciences Division, Fred Hutch Cancer Research Center, Seattle WA
[3]Division of Allergy and Infectious Diseases, Department of Medicine, University of Washington, Seattle WA
[4]Department of Laboratory Medicine and Pathology, University of Washington, Seattle WA
[5]Department of Epidemiology, University of North Carolina at Chapel Hill, Chapel Hill, NC
[6]Department of Microbiology and Immunology, School of Medicine, University of North Carolina at Chapel Hill, Chapel Hill, NC
[7]Vir Biotechnology, San Francisco, CA
[8]Duke Human Vaccine Institute, Duke University School of Medicine, Durham, NC
[9]Department of Surgery, Duke University, Durham, NC

[10]Department of Population Health Sciences, Albany College of Pharmacy and Health Sciences, Albany, NY

*Anton M. Sholukh and Andrew Fiore-Gartland contributed equally to this work. AMS is listed first as co-first author due to contribution to the study design and revision of the manuscript.

[#]Address correspondence to Anton M. Sholukh, asholukh@fredhutch.org and Lawrence Corey, lcorey@fredhutch.org

ABSTRACT

Determinants of protective immunity against SARS-CoV-2 infection require the development of well-standardized, reproducible antibody assays. This need has led to the emergence of a variety of neutralization assays. Head-to-head evaluation of different SARS-CoV-2 neutralization platforms could facilitate comparisons across studies and laboratories. Five neutralization assays were compared using forty plasma samples from convalescent individuals with mild-to-moderate COVID-19: four cell-based systems using either live recombinant SARS-CoV-2 or pseudotyped viral particles created with lentivirus (LV) or vesicular stomatitis virus (VSV) packaging and one surrogate ELISA-based test that measures inhibition of the spike protein receptor binding domain (RBD) binding its receptor, human angiotensin converting enzyme 2 (hACE2). Vero, Vero E6, HEK293T expressing hACE2, and TZM-bl cells expressing hACE2 and transmembrane serine protease 2 were tested. All cell-based assays showed 50% neutralizing dilution (ND50) geometric mean titers (GMTs) that were highly correlated (Pearson r = 0.81–0.89) and ranged within 3.4-fold. The live-virus assay and LV-pseudovirus assays with HEK293T/hACE2 cells showed very similar mean titers: 141

and 178, respectively. ND50 titers positively correlated with plasma IgG targeting SARS-CoV-2 spike and RBD (r = 0.63–0.89), but moderately correlated with nucleoprotein IgG (r = 0.46–0.73). ND80 GMTs mirrored ND50 data and showed similar correlation between assays and with IgG concentrations. The VSV-pseudovirus assay and LV-pseudovirus assay with HEK293T/hACE2 cells in low and high-throughput versions were calibrated against the WHO SARS-CoV-2 IgG standard. High concordance between the outcomes of cell-based assays with live and pseudotyped virions enables valid cross-study comparison using these platforms. 249

INTRODUCTION

The coronavirus disease 2019 (COVID-19) pandemic, caused by severe acute respiratory syndrome coronavirus 2 (SARS-CoV-2), has caused more than 100 million confirmed infections and over 2.4 million deaths worldwide as of February 15, 2021 (https://www.worldometers.info/coronavirus). Despite governmental regulations designed to minimize virus transmission and reduce mortality, such as mask use and social distancing guidelines, vaccines are required to limit the spread of the virus and the burden of COVID-19.

Most efficacious licensed vaccines would elicit pathogen-neutralizing antibodies (nAb) (1). Humans can mount nAb responses against SARS-CoV-2 during natural infection (2–5). Epidemiologic data suggest that reinfection rates are low, albeit increasing numbers of sporadic reinfections are being reported (6, 7). A crucial unknown at this time is what immune responses are associated with protective immunity. While there is mixed evidence supporting the efficacy of convalescent sera infusion for disease shortening, recent studies suggest passive infusion of monoclonal antibodies can alter COVID-19 progression (8, 9). In order to

68 determine what constitutes protective immunity, well-standardized, reproducible antibody
69 assays are required to establish correlates of risk and protection. Efficacy data for several
70 SARS-CoV-2 vaccines have been already published but analyses of correlates of protection
71 are yet to come (10–12). For that, massive serological measurements including virus
72 neutralization are under way. In this regard, it is important to understand how results obtained
73 with different virus neutralization platforms can be compared.

74 The plaque reduction neutralization test (PRNT) is considered a “gold standard” to assess
75 virus neutralizing potency of a serum or antibody sample. However, a variety of live-virus
76 neutralization assays that use recombinant SARS-CoV-2 (rSARS-CoV-2) containing a reporter
77 gene at the *ORF7* locus of the viral genome have been suggested as alternatives (13, 14).
78 These recombinant viruses replicate similarly to SARS-CoV-2 clinical isolates in vitro and
79 successfully infect primary airway epithelial cell cultures. A fluorescence-based rSARS-CoV-2
80 neutralization assay yielded comparable results to PRNT in nAb detection from convalescent
81 patient plasma (13). With a shorter turnaround time (24-48 hours for reporter virus vs. 3 days
82 for PRNT), rSARS-CoV-2 provides a useful high-throughput (HTS) platform to study nAb
83 responses; but unfortunately still requires biosafety level 3 (BSL-3) containment for assay set-
84 up and readout.

85 Reporter assays with pseudotyped viruses restricted to a single round of replication allow nAb
86 experiments to be carried out in BSL-2 laboratories. Pseudotyped viral particles created with
87 lentivirus (LV) and vesicular stomatitis virus (VSV) (15–18) packaging platforms have already
88 been adapted for SARS-CoV-2 (19–21). Several cell lines endogenously or exogenously
89 expressing angiotensin converting enzyme 2 (ACE2), the host receptor for the SARS-CoV-2
90 spike protein, have been tested and Vero cells were among the most susceptible to VSV-

pseudovirus entry (22–24). HEK 293T cells transfected to express ACE2 have also been developed for use in pseudovirus neutralization assays (25). In addition to ACE2, transmembrane serine protease 2 (TMPRSS2) has been shown to prime the spike protein for viral cell entry (24).

Because the receptor binding domain (RBD) of the spike protein is the major target for nAbs (26–28), surrogate, ELISA-based assays were introduced to evaluate antibodies that compete with ACE2 for RBD binding (20, 29, 30). Major advantages of these assays include low cost, speed and safety. As opposed to measuring actual virus neutralization, surrogate assays report percent binding inhibition between RBD and ACE2, which is then interpreted as percent neutralization. While they provide inexpensive and rapid detection of RBD-targeting nAbs, surrogate assays cannot measure neutralization via non-RBD spike protein epitopes. The importance of this issue has increased with the increasing prevalence of escape resistant variants of SARS CoV-2 (31–33) (https://www.cdc.gov/coronavirus/2019-ncov/cases-updates/variant-surveillance/variant-info.html).

The global pandemic led to the unprecedented rapid development and implementation of many SARS-CoV-2 neutralization assays. However, inter-assay comparison and validation is needed to better understand antibody kinetics and longevity of humoral immune responses, correlates of immune protection, and vaccine efficacy (34). In the current study, we aimed to fill this gap by evaluating the same set of plasma samples from convalescent individuals with mild-to-moderate COVID-19 disease with five SARS-CoV-2 neutralization assays including: 1) a live rSARS-CoV-2 assay on Vero E6 cells; 2) VSV pseudotyped with SARS-CoV-2 spike on Vero cells; 3) LV pseudotyped with SARS-CoV-2 spike on HEK293T cells expressing hACE2 in a regular and HTS format; 4) LV-pseudovirus on TZM-bl cells expressing hACE2 and

TMPRSS2; and 5) a surrogate, ELISA-based test that measures inhibition of binding between RBD and ACE2. We also examined the correlation between neutralization and the plasma concentration of SARS-CoV-2 nucleoprotein-, spike- and RBD-specific IgG.

METHODS

Detailed description of reagents and procedures is available in Supplementary Methods.

Study population & specimen collection. Plasma samples used for this study were obtained from participants (≥18 years of age) of a seroepidemiology study following a county-wide outbreak of SARS-CoV-2 in Blaine County, Idaho, in March-April 2020. Study participants were randomly selected after stratification by ZIP code, and within ZIP code, age, gender and race/ethnicity. All volunteers signed electronic consent forms. Demographic information and symptom histories since January 15, 2020 were collected.

Blood was collected in 10 mL vials with acid citrate dextrose and shipped overnight to the laboratory (Fred Hutch, Seattle, WA) where plasma was separated by centrifugation. One aliquot was submitted for the Architect SARS-CoV-2 IgG assay (Abbott, Abbott Park, IL). Other aliquots were heat inactivated for 30 min at 56º C, frozen at -80º C and distributed to testing laboratories for SARS-CoV-2 neutralization assays. Study participants were informed of the qualitative results of the IgG serology assay via email within one week of obtaining test results. This study was approved by the Fred Hutchinson Cancer Research Center Institutional Review Board and all study materials were provided in both English and Spanish.

Cell lines. Vero cells (CCL-81™, ATCC Manassas, VA) are kidney epithelial cells of *Cercopithecus aethiop*s; Vero E6 (CRL-1586™, ATCC) is a cloned variant of Vero cells. Human embryonic kidney cells (CRL-3216™, ATCC), HEK293T, expressing hACE2 (293T/ACE2.MF) were kindly provided by Drs. Mike Farzan and Huihui Mu at Scripps (La Jolla, CA). TZM-bl cells (also called JC53BL-13; NIH AIDS Research and Reference Reagent Program, Cat. no. 8129) are a HeLa cell derivative engineered by amphotropic retroviral transduction to express CD4, CXCR4 and CCR5 (35) and to contain Tat-responsive reporter genes for firefly luciferase (Luc) and *Escherichia coli* β-galactosidase (36), and additionally engineered to express both ACE2 and TMPRSS2 (TZM-bl/ACE2/TMPRSS2 cells), and were kindly provided by Drs. Mike Farzan and Huihui Mu at Scripps.

Viruses. All assays were performed in BSL-2 conditions unless noted differently.

Live SARS-CoV-2. Live recombinant SARS-CoV-2-nanoLuc virus (rSARS-CoV-2-nLuc) was prepared as described elsewhere (14).

VSV-pseudovirus was prepared using a codon-optimized SARS-CoV-2 spike protein (YP_009724390.1) and VSV(G*ΔG-luciferase) system purchased from Kerafast (Boston, MA) (18, 37). VSV(G*ΔG-luciferase) pseudotyped with SARS-CoV-2 spike (PsVSV-Luc-D19) was produced in 293T cells and stored at -80º C. Median tissue culture infectious dose ($TCID_{50}$) was measured using Vero cells (catalog number CCL-81; ATCC) with serial 2-fold dilutions of the prepared pseudovirus.

*LV-pseudoviruses***.** An expression plasmid encoding codon-optimized full-length spike of the Wuhan-1 strain (VRC7480) was provided by Drs. Barney Graham and Kizzmekia Corbett at the Vaccine Research Center, National Institutes of Health (USA). The D614G mutation was

Journal of Clinical Microbiology

introduced into VRC7480 by site-directed mutagenesis using the QuikChange Lightning Site-Directed Mutagenesis Kit (Agilent Technologies, Santa Clara, CA) (LV-pseudo). Pseudovirions were produced in HEK 293T/17 cells (CRL-11268; ATCC). Culture supernatants from transfections were clarified of cells by low-speed centrifugation and filtration (0.45 µm filter) and stored in 1 mL aliquots at -80^{o} C.

For HTS format of the LV-pseudovirus assay, the pseudovirus was prepared in 293T cells using a five-plasmid system as described in (38). Lentiviral backbone plasmids and SARS-CoV-2 spike (Wuhan-1, D614G) vector were provided by Dr. Jessy Bloom at Fred Hutch.

Detection of IgG antibodies to SARS-CoV-2 using a commercial serologic assay. Plasma samples were tested at the Clinical Laboratory Improvement Amendments (CLIA)-certified University of Washington Virology lab using the Architect SARS-CoV-2 IgG assay (Abbott) under the Food and Drug Administration's Emergency Use Authorization. The assay is a chemiluminescent microparticle immunoassay that measures IgG antibodies to the SARS-CoV-2 nucleocapsid protein. Qualitative results and index values reported by the instrument were used in analyses. Recommended index value cutoff of 1.40 was used for determining positivity (39).

Luminex SARS-CoV-2 IgG binding antibody assay. Detailed description can be found in Supplementary Methods. Two replicate dilutions of plasma were incubated with MagPlex beads conjugated with SARS-CoV-2 spike, RBD, nucleoprotein and tetanus toxoid followed by incubation with anti-human IgG Fc-PE (Southern Biotech, Birmingham, AL). Background was established by measuring the mean fluorescence intensity (MFI) of beads conjugated to antigens incubated in assay buffer and subtracted from all readings. Pooled sera from normal

Journal of Clinical Microbiology

human donors collected in 2015–2016 was included as the negative control for SARS-CoV-2 antigens. Convalescent plasma from a subject with PCR-confirmed severe COVID-19 was used as a positive control.

Concentration of antigen-specific IgG was estimated using a standard curve based on the measurement of MFI for serial dilutions of standard IgG (Sigma, St. Louis, MO) captured by MagPlex beads conjugated with anti-Fab anti-human IgG Fab-specific (Southern Biotech). MFI readings and associated IgG concentrations were fitted to a four-parameter logistic curve (4PL) using the R packages *nCal* and *drc*.

Live SARS-CoV-2 neutralization assay. All the live virus experiments were performed under BSL-3 conditions at negative pressure, by operators in Tyvek suits wearing personal powered-air purifying respirators. Vero E6 cells were seeded at $2x10^4$ cells/well in a 96-well plate 24 h before the assay was performed. An 8-point, 3-fold dilution curve was generated for each sample with a starting concentration of 1:50. Seventy-five plaque forming units (pfu) of rSARS-CoV-2-nLuc (14) were mixed with individual patient plasma at 1:1 ratio and incubated at 37º C for 1 h after that virus was added to cells and incubated at 37º C in 5% CO_2 for 48 h. Luciferase was measured as relative luminescence units (RLU) by Nano-Glo Luciferase Assay System (Promega, Madison, WI) following manufacturer protocols using a SpectraMax M3 luminometer (Molecular Devices, San Jose, CA). Percent neutralization was calculated by the following equation: [1-(RLU with sample/RLU with mock treatment)] x 100. Mouse serum produced by BALB/c mice immunized with SARS-CoV-2 spike was used as a positive control (14).

VSV pseudovirus neutralization assay. Vero cells were seeded at $2x10^4$ cells/well in black-walled 96-well plates 24 h before the assay was performed. A 7-point, 3-fold dilution curve was generated with a starting sample dilution of 1:20. PsVSV-Luc-D19 ($3.8x10^2$ TCID50) was mixed with the plasma dilutions, incubated at 37º C in 5% CO_2 for 30 minutes and then transferred onto Vero cells. Cells were incubated for 18-20 h. Luciferase activity was measured by Bio-Glo Luciferase Assay System (Promega) using a 2030 VICTOR X3 multilabel reader (PerkinElmer, Waltham, MA). Percent virus neutralization was calculated as in the live-virus assay. Plasma collected from a subject with severe, PCR-confirmed SARS-CoV-2 infection collected after the person was released from the hospital was used as a positive control. Pooled human serum collected in 2015–2018 was used as a negative control.

LV-pseudovirus neutralization assays.

293T/ACE2 cells pseudovirus assay. A pre-titrated dose of LV-pseudo was incubated with serial 3-fold dilutions of plasma in duplicate for 1 h at 37º C in 96-well plates. Freshly trypsinized 10^4 293T/ACE2 cells were added to each well. One set of control wells received cells + virus (virus control) and another set received cells only (background control). After 68-72 h of incubation, 100 µl of cell lysate was transferred to a 96-well plate for measurements of luminescence using the Promega Luciferase Assay System (Promega).

ACE2/TMPRSS2 TZM-bl cells pseudovirus assay. The assay was carried out similarly to the 293T/ACE2 cell pseudovirus assay with the exception that the growth medium used for infection of TZM-bl/ACE2/TMPRSS2 cells contained 75 µg/ml DEAE dextran. After 68-72 h of incubation, 100 µl of cell lysate was transferred to a 96-well plate (Costar) for luminescence

Journal of Clinical Microbiology

measurement using the BriteLite Luminescence Reporter Gene Assay System (PerkinElmer). Percent virus neutralization was calculated as previously mentioned.

For both LV-pseudovirus assays, SARS-CoV-2 neutralizing monoclonal antibody COVA1-18 (40) was used as a positive control and normal human serum collected in 2016 was used as a negative control.

HTS version of 293T/ACE2 cells pseudovirus assay. HTS SARS-CoV-2 neutralization assay was performed in the CLIA-certified University of Washington Virology lab using Mantis Liquid Handler (Formulatrix, Bedford, MA) to dispense growth media, virus and luciferase substrate. The 293T/ACE2 cells were seeded in 96-well black walled plates manually at 12,500 cells/well and incubated for 16–18 h. Various amounts of growth media were dispensed into 96-well plates using Mantis according to the plate map. In the plates with growth media, patient sera were manually diluted 10-fold followed by six of 3-fold serial dilutions with a total of seven dilution points at 60 µl of sample per well. Mantis was then used to dispense 60 µl of diluted pseudovirus at $4x10^5$ RLU/well into the 96-well plates with serially diluted serum samples. After incubating at 37ºC for 1 h, 100 µl of the pseudovirus and serum mixture was manually added to the 293T/ACE2 cells in 96-well plate. At 52-58 hours post-infection, 100 µl of medium was manually removed from each well and 30 µl of Bright-Glo Luciferase substrate was added by the Mantis. The plates were read with Victor Nivo Multimode Microplate Reader (PerkinElmer).

For all neutralization assays, neutralization titers are the reciprocal of plasma dilution at which RLU were reduced by 50% (ND50) and 80% (ND80) compared to virus control wells after subtraction of background RLUs.

SARS-CoV-2 surrogate virus neutralization test (sVNT). This assay was carried out in a BSL-1 laboratory and was performed according to manufacturer (GenScript, Piscataway, NJ) protocol recommendations. Briefly, capture plates were incubated with plasma samples diluted 1:10, washed and probed with secondary antibody conjugated to horseradish peroxidase. Plates were developed with 3,3',5,5'-tetramethylbenzidine (ThermoFisher, Waltham, MA) and optical density (OD) at 450 nm was measured using SpectraMax M2 reader (Molecular Devices). Positive and negative controls were provided in the kit. Binding inhibition was determined via the following formula: inhibition = (1 – [OD of sample/OD of negative control]) × 100. Percent binding inhibition was interpreted as a percent neutralization. In order to determine ND50, plasma samples were serially diluted starting from 1:10 and the assay was performed as described above.

Assay calibration with the WHO anti-SARS-CoV-2 immunoglobulin standard. The First WHO International Standard for anti-SARS-CoV-2 antibodies developed and distributed by the National Institute for Biological Standards and Control (NIBSC) of the United Kingdom (Cat. # 20/136) was used to establish calibrating factors for VSV-pseudo/Vero, LV-pseudo/293T and HTS-LV-pseudo/293T assays as follows. The lyophilized standard was reconstituted in ultrapure water as per NIBSC instructions. Resulting serum was stored at 4ºC for no longer than one week and was used in the assays similar as described above for patient samples via serial dilutions starting at 1:20. The ratio between the assigned neutralization unitage (1000 IU/ml) and measured ND50 and ND80 for the standard sample was used as a calibrating factor to convert assay-derived ND50 and ND80 readouts into IU/ml.

Statistical analysis and visualization. Neutralization titers were defined as the plasma dilution that reduced RLU by 50% (ND50) or 80% (ND80) relative to virus control wells (cells +

virus only) after subtraction of background RLU in cells-only control wells (see Supplement for details). Correlations were estimated between pairs of neutralization or binding antibody readouts using Pearson's correlation coefficient (*r*) and group means were compared using a paired two-sample *t*-test; measures in units of neutralization and IgG concentration were logged prior to estimating correlation and comparing group means. Association of neutralization and IgG concentration with age and body mass index (BMI) were conducted using Spearman's rank correlation. Statistical significance was based on $p<0.05$.

RESULTS

Cohort characteristics, demographics, survey participation, and serological testing. To characterize and compare different platforms of SARS-CoV-2 nAb assays, we used plasma samples obtained from a seroepidemiology study conducted May 4-19, 2020 following a county-wide outbreak of SARS-CoV-2 in Blaine County, Idaho. Out of 967 participants, 222 (22.8%) had IgG antibodies to SARS-CoV-2 nucleoprotein as measured by the Abbott Architect test (index value ≥1.40) indicative of prior infection with SARS-CoV-2. From these 222 samples, we randomly selected 40 plasma samples for use in evaluating SARS-CoV-2 neutralization assays. Selected participants had a median age of 51.5 years (range, 23-81) and 60% identified as female (**Table 1**). Only one participant reported being hospitalized and four participants (10%) were self-described as asymptomatic. Among participants reporting different symptoms, 57.5% had fever, while fatigue (87.5%), cough (72.5%), headache (67.5%) and chills (65%) were more prevalent (**Table S1**). The majority of participants reported COVID-19 symptoms occurring in March of 2020. Based on this, our cohort can be categorized as representing mild-to-moderate symptomatic COVID-19 infections with samples collected at about 1.5-2 months post disease onset.

We measured the concentration of IgG in participant sera targeting SARS-CoV-2 spike, RBD and nucleoprotein via a quantitative, Luminex-based immunoassay. IgG to tetanus toxoid was measured as a proxy for overall IgG level. IgG to spike and RBD were detected in all forty plasma samples indicating a seroconversion on all SARS-CoV-2 antigens. The mean plasma concentrations for spike- and RBD-specific IgG were 2.8 µg/ml (95%CI: 1.9-4.1) and 2.1 µg/ml (95%CI: 1.4-3.3), respectively, which were considerably lower than those to nucleoprotein (7.3 µg/ml [95%CI: 5.3-10]) (**Fig. 1A**). The concentration of tetanus-specific IgG was higher than IgG targeting SARS-CoV-2 antigens for all individuals (mean 14.5, 95%CI: 11.1-18.9). Although the Abbott SARS-CoV-2 IgG CLIA test is designed and used for qualitative detection of IgG against the SARS-CoV-2 nucleoprotein, the instrument reports index values that can be used in quantitative analyses (**Fig. 1B**) (41).

Cell-based assays provided comparable estimates of neutralization activity. Forty selected plasma samples were distributed across four laboratories conducting different SARS-CoV-2 neutralization assays (**Table 2**). Serial plasma dilutions were used in cell-based assays to generate titration curves (**Fig. S1**) and estimate the 50% and 80% neutralizing dilutions (ND50 and ND80, respectively). In the sVNT, only 22 of 40 samples showed neutralization above 50% when analyzed according to the manufacturer protocol in a single 1:10 dilution (**Fig. S2A**) and 13 samples representing different neutralization capacity were selected for ND50 measurement using serial dilutions (**Fig. S2B**).

Overall, the cell-based assays showed comparable estimated ND50 GMTs with considerable overlap in the interquartile range and 95% CI among pairs of assays (**Fig. 1C, Fig. S3A, Table S2**). The SARS-CoV-2/VeroE6 and LV-pseudo/293T assays yielded very similar ND50 GMT: 141 (95%CI: 93-214) vs 178 (95%CI: 112-283), respectively. The estimated mean ND50 for

other cell-based assays were also comparable, however, ND50 GMT for VSV-pseudo/Vero test and HTS-LV-pseudo/293T were the highest among cell-based assays (310; 95%CI: 211-454 and 272; 95%CI: 267-643, respectively, **Table S2**). The live virus assay and all three LV-pseudovirus assays yielded ND50 within a 2-fold range, indicating high concordance. Notably, rSARS-CoV-2-nLuc and PsVSV-Luc-D19 contained the spike protein with an aspartate residue at position 614 (Wuhan-1 strain), while the LV-pseudoviruses contained spike protein with the D614G mutation. Nevertheless, the difference between outcomes of LV-pseudo/293T assays in regular and HTS formats and VSV-pseudo/Vero assay were within 2-fold. The lowest ND50 GMT (from the LV-pseudo/TZM-bl assay) was 3.4-fold lower than that of the highest yielding assay (VSV-pseudo/Vero).

Despite overlapping distributions, it was possible to detect shifts in ND50 for each cell-based assay using a two-sample, paired t-test ($p<0.05$); the exceptions were SARS-CoV-2/VeroE6 vs. LV-pseudo/293T and HTS-LV-pseudo/293T vs. VSV-pseudo/Vero. The ND50 GMTs in these two assay pairs were not significantly different ($p=0.112$ and 0.856 respectively). Taken together, these data demonstrate that the variability across different cell-based assays is low and it suggests that results of cell-based assays could be adjusted for head-to-head comparability as we show more in the next section. In contrast, the sVNT yielded significantly different ND50s, up to 26-fold lower compared to cell-based assays.

Differences and similarities among the cell-based assay ND50s were generally recapitulated using the ND80s (**Fig. 1D, Fig. S3B, Table S2)**. The sVNT and VSV-pseudo/Vero assays yielded the lowest and the highest ND80 GMTs, respectively. However, the overall difference between ND80 values was less dramatic than for ND50. For all cell-based assays, it was within 3-fold range and sVNT ND80 was only 6–17-fold lower compared to cell-based assays.

As expected, the ND80 titers were consistently lower than the ND50 (**Fig. S4, Table S3**). For other pseudovirus assays, the difference between ND50 and ND80 was greater and ranged between 3 and 4.6-fold (**Table S3**). Interestingly, the live-virus assay showed the smallest difference between ND50 and ND80 GMTs: 1.95-fold (**Table S3**), a direct consequence of the steeper titration curves observed for this assay (**Fig. S1A**). Indeed, the slope parameter from the live-virus neutralization curves was higher than in other assays (slope B = 3.3 vs. 0.6, 1.4, 1.5 for LV-pseudo/293T, LV-pseudo/TZM-bl and VSV-pseudo/Vero, respectively; all p<0.001).

The neutralization assay response rate was in agreement with estimated ND50 and ND80 values. The highest response rates came from the VSV-pseudo/Vero assay (100% of ND50 and 97.5% of ND80 titers) and HTS-LV-pseudo/293 assays (100% of ND50 and ND80 titers) (**Fig. 1C and 1D**). The lowest response rate among the cell-based assays was measured via the SARS-CoV-2/VeroE6 assay, and the sVNT was the lowest overall. For the SARS-CoV-2/VeroE6 assay, the lower response rate compared to other cell-based assays could be due to the starting plasma dilution, which was 1:50 vs 1:20 used in the pseudovirus assays.

Strong correlation among neutralization assays. We conducted a correlation analysis of the ND50 and ND80 values derived from each of the five neutralization assays (**Fig. 2, Fig. S5**). The live-virus and all four pseudovirus neutralization assays generated ND50 values that were highly correlated across samples (Pearson r = 0.78–0.89), with the highest correlation observed between the three LV-pseudovirus assays (r = 0.89, 95%CI: 0.81-0.94, p<0.001). The readout with the lowest correlation with the cell-based assays was the sVNT ND50 (r = 0.32–0.6), though sVNT percent neutralization tended to be more highly correlated (r = 0.73–0.8). Similar correlations were observed for ND80 outcomes for cell-based assays (r = 0.69–0.88) **(Fig. 2B**).

Plasma neutralization potency correlated with concentration of SARS-CoV-2 binding IgG. Correlation analyses revealed a strong association between levels of IgG to spike and RBD (r = 0.89, 95%CI: 0.81-0.94) (**Fig. 2**). Luminex immunoassay-measured nucleoprotein-specific IgG highly correlated with the quantitative index of the Abbott SARS-CoV-2 IgG assay (r = 0.95, 95%CI: 0.91-0.97), which is based on detection of nucleoprotein-specific IgG. but both parameters only moderately correlated with IgG targeting the other viral antigens (r = 0.58–0.68). There was no significant correlation between tetanus-specific IgG and IgG to SARS-CoV-2 antigens (all p>0.05).

Next, we examined the relationship between virus neutralization and IgG levels to spike, RBD and nucleoprotein. IgG concentrations to each antigen positively correlated with the ND50 titer measured by each neutralization assay (r=0.46–0.83) (**Fig. 2A, Fig. S6**). The strongest correlation was observed between sVNT percent neutralization and concentration of RBD IgG (r = 0.89). Among the cell-based assays, the live-virus ND50 titer showed the strongest correlation with IgG against spike and RBD (r=0.83 for both), followed by the VSV-pseudovirus/Vero assay (r=0.83 and 0.76, respectively). Notably, nucleoprotein-specific IgG only moderately correlated with ND50 titers from the cell-based assays, but showed a strong correlation with sVNT percent neutralization. Tetanus-specific IgG did not correlate with any of the SARS-CoV-2-associated IgG concentrations or neutralization titers.

With the caveat that our cohort is rather small for such analyses, we found a moderately positive correlation between age and concentration of spike-specific IgG (Spearman's rho=0.37, p=0.02), RBD-specific IgG (rho=0.39, p=0.013) and nucleoprotein-specific IgG (rho=0.45, p=0.003) (**Table S4**). Similarly, there were positive correlations between age and

neutralization titer (**Table S4**, **Fig. S7**), though the correlations tended to be higher with ND80 (rho=0.51, p=0.001) compared to ND50 titer (rho=0.28, p=0.075).

Assay calibration with the WHO anti-SARS-CoV-2 immunoglobulin standard. To evaluate readout conversion between assays, we calibrated VSV-pseudo/Vero, LV-pseudo/293T and HTS-LV-pseudo/293T using the First WHO International Standard for anti-SARS-CoV-2 antibodies (**Table 3**). After conversion, the regular and HTS version of the LV-pseudo assay reported the same ND50 GMT of 58.4 IU/ml. Of note, raw ND50 titers for these assays also showed high concordance and had a less than 2-fold difference. GMT ND50 from the VSV-pseudo/Vero assay was found at 205 IU/ml after calibration. If before calibration the difference in ND50 titers was about 2-fold between VSV and LV-pseudovirus assays, after calibration it increased up to 3.5-fold. Conversion of ND80 GMTs into IU/ml format produced perplexing results. ND80 value after calibration became greater than ND50 for both LV-pseudo assays and was almost equal to ND50 for VSV-pseudo assay (**Table 3**).

To provide context for our data we accessed the WHO report that established their reference standard (42) and analyzed the GMTs that were contributed by different research groups using a range of assays and reference samples. We pooled together measurements from LV-pseudovirus and VSV-pseudovirus assays and calculated their respective ND50 GMT. Of note, most of the LV- and VSV-pseudovirus assays used for establishing the WHO standard contained the Wuhan-1 D614 spike (42). The calculated GMT for the WHO standard was 1347 for the VSV-pseudovirus assay and 3406 for the LV-pseudovirus assay and were similar to the cognate values from our study (**Table 3**).

To test possible influence of D614G mutation on the assay readout we tested VSV-pseudovirus carrying D614 vs. G614 using the WHO standard and found no difference in ND50 or ND80 titers between virus variants (**Fig. S8**). Therefore, the difference in readouts between VSV and LV platform is either due to the target cells or the virus used for pseudotyping.

Discussion

In this study, we conducted a detailed comparison of four cell-based and one ELISA-based SARS-CoV-2 neutralization assays using a set of 40 plasma samples collected from SARS-CoV-2 convalescent individuals with mild-to-moderate disease. Our data show a high level of congruency among cell-based assays, suggesting that the results obtained with any of the tested pseudovirus platforms accurately reflect the potency of the sample to neutralize the Wuhan-Hu-1 strain of SARS-CoV-2. The 50% and 80% neutralization titers strongly correlate between different assays as well as between the neutralization assays and plasma concentration of RBD and spike-specific IgG, which is consistent with other studies (19, 43–47). Although the correlation was modest in comparison, the ELISA-based sVNT results also positively correlated with the other neutralization assays. The demonstrated differences in ND50 and ND80 GMTs between assays should be considered when conducting SARS-CoV-2 natural history studies and vaccine trials.

Although levels of spike-specific IgG highly correlated with neutralization, our data do not confirm that all IgG targeting the spike protein have neutralization activity. Rather, the results imply that individuals who produce spike-specific binding antibodies are also likely to make

neutralizing IgG. The correlation between nucleoprotein-specific IgG and neutralization was consistently lower than the correlations between spike- and RBD-specific IgG with neutralization. This is not surprising, as much of the immunodominant response associated with neutralization involves binding and/or blocking the spike RBD to inhibit viral entry to host cells (26, 48, 49).

The association of age with both spike-specific IgG and neutralization titer suggests that the previously reported association of high neutralization titer among older individuals may be mediated by higher concentrations of spike and RBD-specific IgG (50, 51). However, this is not a result of cross-reactive humoral responses to prior infections with seasonal coronaviruses (52, 53). Whether this is a direct effect of age on the developing immune response to SARS-CoV-2 or result of cross-reacting T-cell immunity remains unclear (54, 55). Although our cohort was well-balanced by sex and age and a positive correlation between age and neutralizing titers was detected, the influence of other demographic and environmental factors cannot be excluded due to a small sample size collected in a limited geographic origin (56, 57). As such, larger, geographically distinct cohorts are required for proper analyses as, for example, a recent publication showing good congruency across geographically distant laboratories with the VSV-pseudovirus assay (58).

Our study shows that ELISA-based surrogate assays have two major limitations: i) inability to account for synergistic action of antibodies targeting different epitopes; and ii) limits detection to only antibodies that block the RBD/ACE2 interaction, thus missing other antibodies that neutralize via non-RBD sites on the virus glycoprotein (27, 59). In fact, synergistic action of antibodies targeting the RBD and S2 domain has been reported (60). Thus, surrogate assays have a lower sensitivity than cell-based assays and can lead to more false negative results.

These results contradict the use of sVNT as a rapid assay to select positive samples for further screening with cell-based assays, as was recently suggested (61).

TMPRSS2 was shown to be essential for SARS-CoV-2 infectivity of different cell types, although there was no significant difference observed in virus titer at 48 hours post-infection between wildtype Vero cells and Vero cells expressing furin (14, 24). Our comparison revealed that the presence of TMPRSS2 is not critical for assay performance, as TZM-bl cells expressing both ACE2 and TMPRSS2 showed no significant difference compared to 293T cells expressing only ACE2.

In addition to lower safety requirements than assays using replication-competent SARS-CoV-2, pseudotyped virus assays are well positioned for HTS testing of antibody responses elicited by natural infection, vaccination, and now, critically, to new viral variants of concern (VOC), as reported for other viruses (62–64). One limitation of the current study was that only two strains, Wuhan and D614G, were tested. The D614G mutation has been shown to be moderately more susceptible to neutralization (65, 66) while in other reports no difference was observed (67, 68). Our results indicate no pattern between D614G and neutralization capability, and thus the marginal differences observed between assays are likely due to assay sensitivity rather than viral sequence. Neutralization of recently emerging VOCs (69) by serum and monoclonal antibodies has been measured using several assay platforms (70–72); however, assay standardization and validation will be required for proper comparisons.

Use of the First WHO International Standard for anti-SARS-CoV-2 immunoglobulin clearly demonstrated that ND50 GMTs measured with the same assay platform in different laboratories and at different throughputs are highly concordant despite pseudotyped virions

using different spike proteins. However, comparisons across assay platforms is not straightforward and the discordance of GMTs between LV-pseudovirus and VSV-pseudovirus neutralization even after calibration demonstrates that direct conversion from one to the other may require further calibration using multiple samples covering a broad range of neutralization potency.

Compliance with Good Clinical Laboratory Practices is required to ensure that assay results are as reliable as possible (73). Therefore, further assay optimization and subsequent validation addressing how a range of test conditions affect assay specificity, precision, linearity, accuracy, limit of detection, limit of quantitation, and robustness will be required before all or one of the methods evaluated in our study will be transferable between laboratories and suitable for even greater throughput in a 384-well format used for clinical trial testing (64, 74, 75).

SARS-CoV-2 is predicted to remain circulating in the global population for many years due to emerging new strains and incomplete vaccine delivery and uptake (76). Therefore, monitoring of acute and convalescent infection and the broad spectrum of immunity against SARS-CoV-2 both in natural infection and after vaccination will become a routine task for clinical microbiology/virology facilities. Selection of a SARS-CoV-2 neutralization assay and the ability to compare results obtained using different assays will remain a crucial issue.

Acknowledgements

We thank Bill McLaughlin, Hollie Bearce and Dr. Terry O'Connor for sample collection and Sara Thiebaud for assistance with data management and analysis. This work was funded by:

488 NIAID Service Agreement 225472-99 to RKS, R01AI134878 and UM1AI068614 to LC, Fred
489 Hutch Evergreen grant to AMS. HK, AP and FAP are employees of Vir Biotechnology and may
490 hold shares in Vir Biotechnology. LC is a founder of Vir Biotechnologies. The remaining
491 authors declare that the research was conducted in the absence of any commercial or financial
492 relationships that could be construed as a potential conflict of interest.
493

References

1. Plotkin SA. 2010. Correlates of protection induced by vaccination. Clin Vaccine Immunol 17:1055–1065.

2. Greaney AJ, Starr TN, Gilchuk P, Zost SJ, Binshtein E, Loes AN, Hilton SK, Huddleston J, Eguia R, Crawford KH, Dingens AS, Nargi RS, Sutton RE, Suryadevara N, Rothlauf PW, Liu Z, Whelan SP, Carnahan RH, Crowe Jr JE, Bloom JD. Complete mapping of mutations to the SARS-CoV-2 spike receptor-binding domain that escape antibody recognition.

3. Wu F, Wang A, Liu M, Wang Q, Chen J, Xia S, Ling Y, Zhang Y, Xun J, Lu L, Jiang S, Lu H, Wen Y, Huang J. 2020. Neutralizing Antibody Responses to SARS-CoV-2 in a COVID-19 Recovered Patient Cohort and Their Implications. SSRN Electron J 2020.03.30.20047365.

4. Huang AT, Garcia-Carreras B, Hitchings MDT, Yang B, Katzelnick LC, Rattigan SM, Borgert BA, Moreno CA, Solomon BD, Trimmer-Smith L, Etienne V, Rodriguez-Barraquer I, Lessler J, Salje H, Burke DS, Wesolowski A, Cummings DAT. 2020. A systematic review of antibody mediated immunity to coronaviruses: kinetics, correlates of protection, and association with severity. Nat Commun 2020 111 11:1–16.

5. Long QX, Liu BZ, Deng HJ, Wu GC, Deng K, Chen YK, Liao P, Qiu JF, Lin Y, Cai XF, Wang DQ, Hu Y, Ren JH, Tang N, Xu YY, Yu LH, Mo Z, Gong F, Zhang XL, Tian WG, Hu L, Zhang XX, Xiang JL, Du HX, Liu HW, Lang CH, Luo XH, Wu SB, Cui XP, Zhou Z, Zhu MM, Wang J, Xue CJ, Li XF, Wang L, Li ZJ, Wang K, Niu CC, Yang QJ, Tang XJ, Zhang Y, Liu XM, Li JJ, Zhang DC, Zhang F, Liu P, Yuan J, Li Q, Hu JL, Chen J, Huang

AL. 2020. Antibody responses to SARS-CoV-2 in patients with COVID-19. Nat Med 26:845–848.

6. Larson D, Brodniak SL, Voegtly LJ, Cer RZ, Glang LA, Malagon FJ, Long KA, Potocki R, Smith DR, Lanteri C, Burgess T, Bishop-Lilly KA. 2020. A Case of Early Re-infection with SARS-CoV-2. Clin Infect Dis an Off Publ Infect Dis Soc Am.

7. To KK-W, Hung IF-N, Ip JD, Chu AW-H, Chan W-M, Tam AR, Fong CH-Y, Yuan S, Tsoi H-W, Ng AC-K, Lee LL-Y, Wan P, Tso E, To W-K, Tsang D, Chan K-H, Huang J-D, Kok K-H, Cheng VC-C, Yuen K-Y. 2020. COVID-19 re-infection by a phylogenetically distinct SARS-coronavirus-2 strain confirmed by whole genome sequencing. Clin Infect Dis.

8. Weinreich DM, Sivapalasingam S, Norton T, Ali S, Gao H, Bhore R, Musser BJ, Soo Y, Rofail D, Im J, Perry C, Pan C, Hosain R, Mahmood A, Davis JD, Turner KC, Hooper AT, Hamilton JD, Baum A, Kyratsous CA, Kim Y, Cook A, Kampman W, Kohli A, Sachdeva Y, Graber X, Kowal B, DiCioccio T, Stahl N, Lipsich L, Braunstein N, Herman G, Yancopoulos GD. 2020. REGN-COV2, a Neutralizing Antibody Cocktail, in Outpatients with Covid-19. N Engl J Med.

9. Levi-Schaffer F, de Marco A. 2021. COVID-19 and the revival of passive immunization: Antibody therapy for inhibiting SARS-CoV-2 and preventing host cell infection: IUPHAR review: 31. Br J Pharmacol.

10. Voysey M, Clemens SAC, Madhi SA, Weckx LY, Folegatti PM, Aley PK, Angus B, Baillie VL, Barnabas SL, Bhorat QE, Bibi S, Briner C, Cicconi P, Collins AM, Colin-Jones R, Cutland CL, Darton TC, Dheda K, Duncan CJA, Emary KRW, Ewer KJ, Fairlie L, Faust SN, Feng S, Ferreira DM, Finn A, Goodman AL, Green CM, Green CA, Heath PT, Hill C,

538 Hill H, Hirsch I, Hodgson SHC, Izu A, Jackson S, Jenkin D, Joe CCD, Kerridge S, Koen
539 A, Kwatra G, Lazarus R, Lawrie AM, Lelliott A, Libri V, Lillie PJ, Mallory R, Mendes AVA,
540 Milan EP, Minassian AM, McGregor A, Morrison H, Mujadidi YF, Nana A, O'Reilly PJ,
541 Padayachee SD, Pittella A, Plested E, Pollock KM, Ramasamy MN, Rhead S,
542 Schwarzbold A V, Singh N, Smith A, Song R, Snape MD, Sprinz E, Sutherland RK,
543 Tarrant R, Thomson EC, Török ME, Toshner M, Turner DPJ, Vekemans J, Villafana TL,
544 Watson MEE, Williams CJ, Douglas AD, Hill AVS, Lambe T, Gilbert SC, Pollard AJ,
545 Aban M, Abayomi F, Abeyskera K, Aboagye J, Adam M, Adams K, Adamson J, Adelaja
546 YA, Adewetan G, Adlou S, Ahmed K, Akhalwaya Y, Akhalwaya S, Alcock A, Ali A, Allen
547 ER, Allen L, Almeida TCDSC, Alves MPS, Amorim F, Andritsou F, Anslow R, Appleby M,
548 Arbe-Barnes EH, Ariaans MP, Arns B, Arruda L, Azi P, Azi L, Babbage G, Bailey C,
549 Baker KF, Baker M, Baker N, Baker P, Baldwin L, Baleanu I, Bandeira D, Bara A,
550 Barbosa MAS, Barker D, Barlow GD, Barnes E, Barr AS, Barrett JR, Barrett J, Bates L,
551 Batten A, Beadon K, Beales E, Beckley R, Belij-Rammerstorfer S, Bell J, Bellamy D,
552 Bellei N, Belton S, Berg A, Bermejo L, Berrie E, Berry L, Berzenyi D, Beveridge A,
553 Bewley KR, Bexhell H, Bhikha S, Bhorat AE, Bhorat ZE, Bijker E, Birch G, Birch S, Bird
554 A, Bird O, Bisnauthsing K, Bittaye M, Blackstone K, Blackwell L, Bletchly H, Blundell CL,
555 Blundell SR, Bodalia P, Boettger BC, Bolam E, Boland E, Bormans D, Borthwick N,
556 Bowring F, Boyd A, Bradley P, Brenner T, Brown P, Brown C, Brown-O'Sullivan C, Bruce
557 S, Brunt E, Buchan R, Budd W, Bulbulia YA, Bull M, Burbage J, Burhan H, Burn A,
558 Buttigieg KR, Byard N, Cabera Puig I, Calderon G, Calvert A, Camara S, Cao M,
559 Cappuccini F, Cardoso JR, Carr M, Carroll MW, Carson-Stevens A, Carvalho Y de M,
560 Carvalho JAM, Casey HR, Cashen P, Castro T, Castro LC, Cathie K, Cavey A, Cerbino-

561 Neto J, Chadwick J, Chapman D, Charlton S, Chelysheva I, Chester O, Chita S, Cho J-
562 S, Cifuentes L, Clark E, Clark M, Clarke A, Clutterbuck EA, Collins SLK, Conlon CP,
563 Connarty S, Coombes N, Cooper C, Cooper R, Cornelissen L, Corrah T, Cosgrove C,
564 Cox T, Crocker WEM, Crosbie S, Cullen L, Cullen D, Cunha DRMF, Cunningham C,
565 Cuthbertson FC, Da Guarda SNF, da Silva LP, Damratoski BE, Danos Z, Dantas MTDC,
566 Darroch P, Datoo MS, Datta C, Davids M, Davies SL, Davies H, Davis E, Davis J, Davis
567 J, De Nobrega MMD, De Oliveira Kalid LM, Dearlove D, Demissie T, Desai A, Di Marco
568 S, Di Maso C, Dinelli MIS, Dinesh T, Docksey C, Dold C, Dong T, Donnellan FR, Dos
569 Santos T, dos Santos TG, Dos Santos EP, Douglas N, Downing C, Drake J, Drake-
570 Brockman R, Driver K, Drury R, Dunachie SJ, Durham BS, Dutra L, Easom NJW, van
571 Eck S, Edwards M, Edwards NJ, El Muhanna OM, Elias SC, Elmore M, English M,
572 Esmail A, Essack YM, Farmer E, Farooq M, Farrar M, Farrugia L, Faulkner B, Fedosyuk
573 S, Felle S, Feng S, Ferreira Da Silva C, Field S, Fisher R, Flaxman A, Fletcher J, Fofie
574 H, Fok H, Ford KJ, Fowler J, Fraiman PHA, Francis E, Franco MM, Frater J, Freire
575 MSM, Fry SH, Fudge S, Furze J, Fuskova M, Galian-Rubio P, Galiza E, Garlant H,
576 Gavrila M, Geddes A, Gibbons KA, Gilbride C, Gill H, Glynn S, Godwin K, Gokani K,
577 Goldoni UC, Goncalves M, Gonzalez IGS, Goodwin J, Goondiwala A, Gordon-Quayle K,
578 Gorini G, Grab J, Gracie L, Greenland M, Greenwood N, Greffrath J, Groenewald MM,
579 Grossi L, Gupta G, Hackett M, Hallis B, Hamaluba M, Hamilton E, Hamlyn J,
580 Hammersley D, Hanrath AT, Hanumunthadu B, Harris SA, Harris C, Harris T, Harrison
581 TD, Harrison D, Hart TC, Hartnell B, Hassan S, Haughney J, Hawkins S, Hay J, Head I,
582 Henry J, Hermosin Herrera M, Hettle DB, Hill J, Hodges G, Horne E, Hou MM, Houlihan
583 C, Howe E, Howell N, Humphreys J, Humphries HE, Hurley K, Huson C, Hyder-Wright

584 A, Hyams C, Ikram S, Ishwarbhai A, Ivan M, Iveson P, Iyer V, Jackson F, De Jager J,
585 Jaumdally S, Jeffers H, Jesudason N, Jones B, Jones K, Jones E, Jones C, Jorge MR,
586 Jose A, Joshi A, Júnior EAMS, Kadziola J, Kailath R, Kana F, Karampatsas K,
587 Kasanyinga M, Keen J, Kelly EJ, Kelly DM, Kelly D, Kelly S, Kerr D, Kfouri R de Á, Khan
588 L, Khozoee B, Kidd S, Killen A, Kinch J, Kinch P, King LDW, King TB, Kingham L,
589 Klenerman P, Knapper F, Knight JC, Knott D, Koleva S, Lang M, Lang G, Larkworthy
590 CW, Larwood JPJ, Law R, Lazarus EM, Leach A, Lees EA, Lemm N-M, Lessa A, Leung
591 S, Li Y, Lias AM, Liatsikos K, Linder A, Lipworth S, Liu S, Liu X, Lloyd A, Lloyd S, Loew
592 L, Lopez Ramon R, Lora L, Lowthorpe V, Luz K, MacDonald JC, MacGregor G,
593 Madhavan M, Mainwaring DO, Makambwa E, Makinson R, Malahleha M, Malamatsho R,
594 Mallett G, Mansatta K, Maoko T, Mapetla K, Marchevsky NG, Marinou S, Marlow E,
595 Marques GN, Marriott P, Marshall RP, Marshall JL, Martins FJ, Masenya M, Masilela M,
596 Masters SK, Mathew M, Matlebjane H, Matshidiso K, Mazur O, Mazzella A, McCaughan
597 H, McEwan J, McGlashan J, McInroy L, McIntyre Z, McLenaghan D, McRobert N,
598 McSwiggan S, Megson C, Mehdipour S, Meijs W, Mendonça RNÁ, Mentzer AJ, Mirtorabi
599 N, Mitton C, Mnyakeni S, Moghaddas F, Molapo K, Moloi M, Moore M, Moraes-Pinto MI,
600 Moran M, Morey E, Morgans R, Morris S, Morris S, Morris HC, Morselli F, Morshead G,
601 Morter R, Mottal L, Moultrie A, Moya N, Mpelembue M, Msomi S, Mugodi Y,
602 Mukhopadhyay E, Muller J, Munro A, Munro C, Murphy S, Mweu P, Myasaki CH, Naik
603 G, Naker K, Nastouli E, Nazir A, Ndlovu B, Neffa F, Njenga C, Noal H, Noé A, Novaes G,
604 Nugent FL, Nunes G, O'Brien K, O'Connor D, Odam M, Oelofse S, Oguti B, Olchawski
605 V, Oldfield NJ, Oliveira MG, Oliveira C, Oosthuizen A, O'Reilly P, Osborne P, Owen
606 DRJ, Owen L, Owens D, Owino N, Pacurar M, Paiva BVB, Palhares EMF, Palmer S,

607 Parkinson S, Parracho HMRT, Parsons K, Patel D, Patel B, Patel F, Patel K, Patrick-
608 Smith M, Payne RO, Peng Y, Penn EJ, Pennington A, Peralta Alvarez MP, Perring J,
609 Perry N, Perumal R, Petkar S, Philip T, Phillips DJ, Phillips J, Phohu MK, Pickup L,
610 Pieterse S, Piper J, Pipini D, Plank M, Du Plessis J, Pollard S, Pooley J, Pooran A,
611 Poulton I, Powers C, Presa FB, Price DA, Price V, Primeira M, Proud PC, Provstgaard-
612 Morys S, Pueschel S, Pulido D, Quaid S, Rabara R, Radford A, Radia K, Rajapaska D,
613 Rajeswaran T, Ramos ASF, Ramos Lopez F, Rampling T, Rand J, Ratcliffe H,
614 Rawlinson T, Rea D, Rees B, Reiné J, Resuello-Dauti M, Reyes Pabon E, Ribiero CM,
615 Ricamara M, Richter A, Ritchie N, Ritchie AJ, Robbins AJ, Roberts H, Robinson RE,
616 Robinson H, Rocchetti TT, Rocha BP, Roche S, Rollier C, Rose L, Ross Russell AL,
617 Rossouw L, Royal S, Rudiansyah I, Ruiz S, Saich S, Sala C, Sale J, Salman AM,
618 Salvador N, Salvador S, Sampaio M, Samson AD, Sanchez-Gonzalez A, Sanders H,
619 Sanders K, Santos E, Santos Guerra MFS, Satti I, Saunders JE, Saunders C, Sayed A,
620 Schim van der Loeff I, Schmid AB, Schofield E, Screaton G, Seddiqi S, Segireddy RR,
621 Senger R, Serrano S, Shah R, Shaik I, Sharpe HE, Sharrocks K, Shaw R, Shea A,
622 Shepherd A, Shepherd JG, Shiham F, Sidhom E, Silk SE, da Silva Moraes AC, Silva-
623 Junior G, Silva-Reyes L, Silveira AD, Silveira MB V, Sinha J, Skelly DT, Smith DC, Smith
624 N, Smith HE, Smith DJ, Smith CC, Soares A, Soares T, Solórzano C, Sorio GL, Sorley
625 K, Sosa-Rodriguez T, Souza CMCDL, Souza BSDF, Souza AR, Spencer AJ, Spina F,
626 Spoors L, Stafford L, Stamford I, Starinskij I, Stein R, Steven J, Stockdale L, Stockwell L
627 V, Strickland LH, Stuart AC, Sturdy A, Sutton N, Szigeti A, Tahiri-Alaoui A, Tanner R,
628 Taoushanis C, Tarr AW, Taylor K, Taylor U, Taylor IJ, Taylor J, te Water Naude R,
629 Themistocleous Y, Themistocleous A, Thomas M, Thomas K, Thomas TM, Thombrayil

630 A, Thompson F, Thompson A, Thompson K, Thompson A, Thomson J, Thornton-Jones
631 V, Tighe PJ, Tinoco LA, Tiongson G, Tladinyane B, Tomasicchio M, Tomic A, Tonks S,
632 Towner J, Tran N, Tree J, Trillana G, Trinham C, Trivett R, Truby A, Tsheko BL, Turabi
633 A, Turner R, Turner C, Ulaszewska M, Underwood BR, Varughese R, Verbart D, Verheul
634 M, Vichos I, Vieira T, Waddington CS, Walker L, Wallis E, Wand M, Warbick D, Wardell
635 T, Warimwe G, Warren SC, Watkins B, Watson E, Webb S, Webb-Bridges A, Webster A,
636 Welch J, Wells J, West A, White C, White R, Williams P, Williams RL, Winslow R,
637 Woodyer M, Worth AT, Wright D, Wroblewska M, Yao A, Zimmer R, Zizi D, Zuidewind P.
638 2021. Safety and efficacy of the ChAdOx1 nCoV-19 vaccine (AZD1222) against SARS-
639 CoV-2: an interim analysis of four randomised controlled trials in Brazil, South Africa,
640 and the UK. Lancet 397:99–111.

641 11. Baden LR, El Sahly HM, Essink B, Kotloff K, Frey S, Novak R, Diemert D, Spector SA,
642 Rouphael N, Creech CB, McGettigan J, Khetan S, Segall N, Solis J, Brosz A, Fierro C,
643 Schwartz H, Neuzil K, Corey L, Gilbert P, Janes H, Follmann D, Marovich M, Mascola J,
644 Polakowski L, Ledgerwood J, Graham BS, Bennett H, Pajon R, Knightly C, Leav B, Deng
645 W, Zhou H, Han S, Ivarsson M, Miller J, Zaks T. 2021. Efficacy and Safety of the mRNA-
646 1273 SARS-CoV-2 Vaccine. N Engl J Med 384:403–416.

647 12. Polack FP, Thomas SJ, Kitchin N, Absalon J, Gurtman A, Lockhart S, Perez JL, Pérez
648 Marc G, Moreira ED, Zerbini C, Bailey R, Swanson KA, Roychoudhury S, Koury K, Li P,
649 Kalina W V, Cooper D, Frenck RW, Hammitt LL, Türeci Ö, Nell H, Schaefer A, Ünal S,
650 Tresnan DB, Mather S, Dormitzer PR, Şahin U, Jansen KU, Gruber WC. 2020. Safety
651 and Efficacy of the BNT162b2 mRNA Covid-19 Vaccine. N Engl J Med 383:2603–2615.

652 13. Muruato AE, Fontes-Garfias CR, Ren P, Garcia-blanco MA, Menachery VD, Xie X, Shi

P, Fontes-gar CR, Ren P, Garcia-blanco MA, Menachery VD, Xie X, Shi P. 2020. A high-throughput neutralizing antibody assay for COVID-19 diagnosis and vaccine evaluation. Nat Commun 11:4059.

14. Hou YJ, Okuda K, Edwards CE, Martinez DR, Asakura T, Dinnon KH, Kato T, Lee RE, Yount BL, Mascenik TM, Chen G, Olivier KN, Ghio A, Tse L V., Leist SR, Gralinski LE, Schäfer A, Dang H, Gilmore R, Nakano S, Sun L, Fulcher ML, Livraghi-Butrico A, Nicely NI, Cameron M, Cameron C, Kelvin DJ, de Silva A, Margolis DM, Markmann A, Bartelt L, Zumwalt R, Martinez FJ, Salvatore SP, Borczuk A, Tata PR, Sontake V, Kimple A, Jaspers I, O'Neal WK, Randell SH, Boucher RC, Baric RS. 2020. SARS-CoV-2 Reverse Genetics Reveals a Variable Infection Gradient in the Respiratory Tract. Cell 1–18.

15. Li Q, Liu Q, Huang W, Li X, Wang Y. 2018. Current status on the development of pseudoviruses for enveloped viruses. Rev Med Virol 28:1–10.

16. Carnell GW, Ferrara F, Grehan K, Thompson CP, Temperton NJ. 2015. Pseudotype-based neutralization assays for influenza: a systematic analysis. Front Immunol 6:161.

17. Zhao G, Du L, Ma C, Li Y, Li L, Poon VKM, Wang L, Yu F, Zheng B-J, Jiang S, Zhou Y. 2013. A safe and convenient pseudovirus-based inhibition assay to detect neutralizing antibodies and screen for viral entry inhibitors against the novel human coronavirus MERS-CoV. Virol J 10:266.

18. Whitt MA. 2010. Generation of VSV pseudotypes using recombinant DeltaG-VSV for studies on virus entry, identification of entry inhibitors, and immune responses to vaccines. J Virol Methods 169:365–374.

19. Yang R, Huang B, A R, Li W, Wang W, Deng Y, Tan W. 2020. Development and

effectiveness of Pseudotyped SARS-CoV-2 system as determined by neutralizing efficiency and entry inhibition test in vitro. Biosaf Heal.

20. Walker SN, Chokkalingam N, Reuschel EL, Purwar M, Xu Z, Gary EN, Kim KY, Helble M, Schultheis K, Walters J, Ramos S, Muthumani K, Smith TRF, Broderick KE, Tebas P, Patel A, Weiner DB, Kulp DW. 2020. SARS-CoV-2 assays to detect functional antibody responses that block ACE2 recognition in vaccinated animals and infected patients. J Clin Microbiol JCM.01533-20.

21. Hoffmann MAG, Bar-On Y, Yang Z, Gristick HB, Gnanapragasam PNP, Vielmetter J, Nussenzweig MC, Bjorkman PJ. 2020. Nanoparticles presenting clusters of CD4 expose a universal vulnerability of HIV-1 by mimicking target cells. Proc Natl Acad Sci 202010320.

22. Matsuyama S, Nao N, Shirato K, Kawase M, Saito S, Takayama I, Nagata N, Sekizuka T, Katoh H, Kato F, Sakata M, Tahara M, Kutsuna S, Ohmagari N, Kuroda M, Suzuki T, Kageyama T, Takeda M. 2020. Enhanced isolation of SARS-CoV-2 by TMPRSS2-expressing cells. Proc Natl Acad Sci 117:7001 LP – 7003.

23. Ren X, Glende J, Al-Falah M, de Vries V, Schwegmann-Wessels C, Qu X, Tan L, Tschernig T, Deng H, Naim HY, Herrler G. 2006. Analysis of ACE2 in polarized epithelial cells: Surface expression and function as receptor for severe acute respiratory syndrome-associated coronavirus. J Gen Virol 87:1691–1695.

24. Hoffmann M, Kleine-Weber H, Schroeder S, Krüger N, Herrler T, Erichsen S, Schiergens TS, Herrler G, Wu NH, Nitsche A, Müller MA, Drosten C, Pöhlmann S. 2020. SARS-CoV-2 Cell Entry Depends on ACE2 and TMPRSS2 and Is Blocked by a Clinically

Proven Protease Inhibitor. Cell 181:271-280.e8.

25. Hu J, Gao Q, He C, Huang A, Tang N, Wang K. 2020. Development of cell-based pseudovirus entry assay to identify potential viral entry inhibitors and neutralizing antibodies against SARS-CoV-2. Genes Dis.

26. Seydoux E, Homad LJ, MacCamy AJ, Parks KR, Hurlburt NK, Jennewein MF, Akins NR, Stuart AB, Wan YH, Feng J, Whaley RE, Singh S, Boeckh M, Cohen KW, McElrath MJ, Englund JA, Chu HY, Pancera M, McGuire AT, Stamatatos L. 2020. Analysis of a SARS-CoV-2-Infected Individual Reveals Development of Potent Neutralizing Antibodies with Limited Somatic Mutation. Immunity 53:98-105.e5.

27. Rogers TF, Zhao F, Huang D, Beutler N, Burns A, He WT, Limbo O, Smith C, Song G, Woehl J, Yang L, Abbott RK, Callaghan S, Garcia E, Hurtado J, Parren M, Peng L, Ramirez S, Ricketts J, Ricciardi MJ, Rawlings SA, Wu NC, Yuan M, Smith DM, Nemazee D, Teijaro JR, Voss JE, Wilson IA, Andrabi R, Briney B, Landais E, Sok D, Jardine JG, Burton DR. 2020. Isolation of potent SARS-CoV-2 neutralizing antibodies and protection from disease in a small animal model. Science (80-) 369:956–963.

28. Ju B, Zhang Q, Ge J, Wang R, Sun J, Ge X, Yu J, Shan S, Zhou B, Song S, Tang X, Yu J, Lan J, Yuan J, Wang H, Zhao J, Zhang S, Wang Y, Shi X, Liu L, Zhao J, Wang X, Zhang Z, Zhang L. 2020. Human neutralizing antibodies elicited by SARS-CoV-2 infection. Nature 584:115–119.

29. Abe KT, Li Z, Samson R, Samavarchi-Tehrani P, Valcourt EJ, Wood H, Budylowski P, Dupuis A, Girardin RC, Rathod B, Colwill K, McGeer A, Mubareka S, Gommerman JL, Durocher Y, Ostrowski M, McDonough KA, Drebot MA, Drews SJ, Rini JM, Gingras A-C,

719 Dupuis Ii AP, Girardin RC, Rathod B, Wang J, Barrios-Rodiles M, Colwill K, McGeer A,
720 Mubareka S, Gommerman JL, Durocher Y, Ostrowski M, McDonough KA, Drebot MA,
721 Drews SJ, Rini JM, Gingras A-C. 2020. A simple protein-based SARS-CoV-2 surrogate
722 neutralization assay. JCI insight.

723 30. Tan CW, Chia WN, Qin X, Liu P, Chen MI-C, Tiu C, Hu Z, Chen VC-W, Young BE, Sia
724 WR, Tan Y-J, Foo R, Yi Y, Lye DC, Anderson DE, Wang L-F. 2020. A SARS-CoV-2
725 surrogate virus neutralization test based on antibody-mediated blockage of ACE2-spike
726 protein-protein interaction. Nat Biotechnol 38:1073–1078.

727 31. Wibmer CK, Ayres F, Hermanus T, Madzivhandila M, Kgagudi P, Lambson BE,
728 Vermeulen M, van den Berg K, Rossouw T, Boswell M, Ueckermann V, Meiring S, von
729 Gottberg A, Cohen C, Morris L, Bhiman JN, Moore PL. 2021. SARS-CoV-2 501Y.V2
730 escapes neutralization by South African COVID-19 donor plasma. bioRxiv Prepr Serv
731 Biol.

732 32. Weisblum Y, Schmidt F, Zhang F, DaSilva J, Poston D, Lorenzi JC, Muecksch F,
733 Rutkowska M, Hoffmann HH, Michailidis E, Gaebler C, Agudelo M, Cho A, Wang Z,
734 Gazumyan A, Cipolla M, Luchsinger L, Hillyer CD, Caskey M, Robbiani DF, Rice CM,
735 Nussenzweig MC, Hatziioannou T, Bieniasz PD. 2020. Escape from neutralizing
736 antibodies 1 by SARS-CoV-2 spike protein variants. Elife 9:1.

737 33. Paola Cristina Resende, João Felipe Bezerra, Romero Henrique Teixeira de
738 Vasconcelos, Ighor Arantes, Luciana Appolinario, Ana Carolina Mendonça, Anna
739 Carolina Paixao, Ana Carolina Duarte Rodrigues, Thauane Silva, Alice Sampaio Rocha,
740 Alx Pauvo MMS. 2021. Spike E484K mutation in the first SARS-CoV-2 reinfection case
741 confirmed in Brazil.

742 34. Gundlapalli A V, Salerno RM, Brooks JT, Averhoff F, Petersen LR, McDonald LC,
743 Iademarco MF. 2021. SARS-CoV-2 Serologic Assay Needs for the Next Phase of the US
744 COVID-19 Pandemic Response. Open forum Infect Dis 8:ofaa555.

745 35. Platt EJ, Wehrly K, Kuhmann SE, Chesebro B, Kabat D. 1998. Effects of CCR5 and CD4
746 Cell Surface Concentrations on Infections by Macrophagetropic Isolates of Human
747 Immunodeficiency Virus Type 1. J Virol 72:2855 LP – 2864.

748 36. Wei X, Decker JM, Liu H, Zhang Z, Arani RB, Kilby JM, Saag MS, Wu X, Shaw GM,
749 Kappes JC. 2002. Emergence of Resistant Human Immunodeficiency Virus Type 1 in
750 Patients Receiving Fusion Inhibitor (T-20) Monotherapy. Antimicrob Agents Chemother
751 46:1896 LP – 1905.

752 37. Zhao X, Howell KA, He S, Brannan JM, Wec AZ, Davidson E, Turner HL, Chiang C-I, Lei
753 L, Fels JM, Vu H, Shulenin S, Turonis AN, Kuehne AI, Liu G, Ta M, Wang Y, Sundling C,
754 Xiao Y, Spence JS, Doranz BJ, Holtsberg FW, Ward AB, Chandran K, Dye JM, Qiu X, Li
755 Y, Aman MJ. 2017. Immunization-Elicited Broadly Protective Antibody Reveals
756 Ebolavirus Fusion Loop as a Site of Vulnerability. Cell 169:891-904.e15.

757 38. Crawford KHD, Eguia R, Dingens AS, Loes AN, Malone KD, Wolf CR, Chu HY, Tortorici
758 MA, Veesler D, Murphy M, Pettie D, King NP, Balazs AB, Bloom JD. 2020. Protocol and
759 Reagents for Pseudotyping Lentiviral Particles with SARS-CoV-2 Spike Protein for
760 Neutralization Assays. Viruses .

761 39. Bryan A, Pepper G, Wener MH, Fink SL, Morishima C, Chaudhary A, Jerome KR,
762 Mathias PC, Greninger AL. 2020. Performance characteristics of the abbott architect
763 sars-cov-2 igg assay and seroprevalence in Boise, Idaho. J Clin Microbiol 58:4–11.

764 40. Brouwer PJM, Caniels TG, van der Straten K, Snitselaar JL, Aldon Y, Bangaru S, Torres
765 JL, Okba NMA, Claireaux M, Kerster G, Bentlage AEH, van Haaren MM, Guerra D,
766 Burger JA, Schermer EE, Verheul KD, van der Velde N, van der Kooi A, van Schooten J,
767 van Breemen MJ, Bijl TPL, Sliepen K, Aartse A, Derking R, Bontjer I, Kootstra NA,
768 Wiersinga WJ, Vidarsson G, Haagmans BL, Ward AB, de Bree GJ, Sanders RW, van
769 Gils MJ. 2020. Potent neutralizing antibodies from COVID-19 patients define multiple
770 targets of vulnerability. Science (80-) 369:643 LP – 650.

771 41. Bryan A, Pepper G, Wener MH, Fink SL, Morishima C, Chaudhary A, Jerome KR,
772 Mathias PC, Greninger AL. 2020. Performance characteristics of the abbott architect
773 sars-cov-2 igg assay and seroprevalence in Boise, Idaho. J Clin Microbiol 58:4–11.

774 42. Mattiuzzo G, Bentley EM, Hassall M, Routley S. 2020. Establishment of the WHO
775 International Standard and Reference Panel for anti-SARS-CoV-2 antibodyWorld Health
776 Organization.

777 43. Amanat F, Stadlbauer D, Strohmeier S, Nguyen THO, Chromikova V, McMahon M,
778 Jiang K, Arunkumar GA, Jurczyszak D, Polanco J, Bermudez-Gonzalez M, Kleiner G,
779 Aydillo T, Miorin L, Fierer DS, Lugo LA, Kojic EM, Stoever J, Liu STH, Cunningham-
780 Rundles C, Felgner PL, Moran T, García-Sastre A, Caplivski D, Cheng AC, Kedzierska
781 K, Vapalahti O, Hepojoki JM, Simon V, Krammer F. 2020. A serological assay to detect
782 SARS-CoV-2 seroconversion in humans. Nat Med 26:1033–1036.

783 44. Padoan A, Zuin S, Cosma C, Basso D, Plebani M, Bonfante F. 2020. Clinical
784 performances of an ELISA for SARS-CoV-2 antibody assay and correlation with
785 neutralization activity. Clin Chim Acta 510:654–655.

786 45. Schmidt F, Weisblum Y, Muecksch F, Hoffmann H-H, Michailidis E, Lorenzi JCC,
787 Mendoza P, Rutkowska M, Bednarski E, Gaebler C, Agudelo M, Cho A, Wang Z,
788 Gazumyan A, Cipolla M, Caskey M, Robbiani DF, Nussenzweig MC, Rice CM,
789 Hatziioannou T, Bieniasz PD. 2020. Measuring SARS-CoV-2 neutralizing antibody
790 activity using pseudotyped and chimeric viruses. J Exp Med 217.

791 46. Case JB, Rothlauf PW, Chen RE, Liu Z, Zhao H, Kim AS, Bloyet LM, Zeng Q, Tahan S,
792 Droit L, Ilagan MXG, Tartell MA, Amarasinghe G, Henderson JP, Miersch S, Ustav M,
793 Sidhu S, Virgin HW, Wang D, Ding S, Corti D, Theel ES, Fremont DH, Diamond MS,
794 Whelan SPJ. 2020. Neutralizing Antibody and Soluble ACE2 Inhibition of a Replication-
795 Competent VSV-SARS-CoV-2 and a Clinical Isolate of SARS-CoV-2. Cell Host Microbe
796 28:475-485.e5.

797 47. Mazzini L, Martinuzzi D, Hyseni I, Benincasa L, Molesti E, Casa E, Lapini G, Piu P,
798 Trombetta CM, Marchi S, Razzano I, Manenti A, Montomoli E. 2021. Comparative
799 analyses of SARS-CoV-2 binding (IgG, IgM, IgA) and neutralizing antibodies from
800 human serum samples. J Immunol Methods 489:112937.

801 48. Robbiani DF, Gaebler C, Muecksch F, Lorenzi JCC, Wang Z, Cho A, Agudelo M, Barnes
802 CO, Gazumyan A, Finkin S, Hägglöf T, Oliveira TY, Viant C, Hurley A, Hoffmann HH,
803 Millard KG, Kost RG, Cipolla M, Gordon K, Bianchini F, Chen ST, Ramos V, Patel R,
804 Dizon J, Shimeliovich I, Mendoza P, Hartweger H, Nogueira L, Pack M, Horowitz J,
805 Schmidt F, Weisblum Y, Michailidis E, Ashbrook AW, Waltari E, Pak JE, Huey-Tubman
806 KE, Koranda N, Hoffman PR, West AP, Rice CM, Hatziioannou T, Bjorkman PJ,
807 Bieniasz PD, Caskey M, Nussenzweig MC. 2020. Convergent antibody responses to
808 SARS-CoV-2 in convalescent individuals. Nature 584:437–442.

809 49. Ju B, Zhang Q, Ge J, Wang R, Sun J, Ge X, Yu J, Shan S, Zhou B, Song S, Tang X, Yu
810 J, Lan J, Yuan J, Wang H, Zhao J, Zhang S, Wang Y, Shi X, Liu L, Zhao J, Wang X,
811 Zhang Z, Zhang L. 2020. Human neutralizing antibodies elicited by SARS-CoV-2
812 infection. Nature 584:115–119.

813 50. Schlickeiser S, Schwarz T, Steiner S, Wittke K, Al Besher N, Meyer O, Kalus U, Pruß A,
814 Kurth F, Zoller T, Witzenrath M, Sander LE, Müller MA, Scheibenbogen C, Volk H-D,
815 Drosten C, Corman VM, Hanitsch LG. 2021. Disease Severity, Fever, Age, and Sex
816 Correlate With SARS-CoV-2 Neutralizing Antibody Responses. Front Immunol
817 11:628971.

818 51. Yang HS, Costa V, Racine-Brzostek SE, Acker KP, Yee J, Chen Z, Karbaschi M, Zuk R,
819 Rand S, Sukhu A, Klasse PJ, Cushing MM, Chadburn A, Zhao Z. 2021. Association of
820 Age With SARS-CoV-2 Antibody Response. JAMA Netw Open 4:e214302.

821 52. Legros V, Denolly S, Vogrig M, Boson B, Siret E, Rigaill J, Pillet S, Grattard F, Gonzalo
822 S, Verhoeven P, Allatif O, Berthelot P, Pélissier C, Thiery G, Botelho-Nevers E, Millet G,
823 Morel J, Paul S, Walzer T, Cosset FL, Bourlet T, Pozzetto B. 2021. A longitudinal study
824 of SARS-CoV-2-infected patients reveals a high correlation between neutralizing
825 antibodies and COVID-19 severity. Cell Mol Immunol 18:318–327.

826 53. Anderson EM, Goodwin EC, Verma A, Arevalo CP, Bolton MJ, Weirick ME, Gouma S,
827 McAllister CM, Christensen SR, Weaver J, Hicks P, Manzoni TB, Oniyide O, Ramage H,
828 Mathew D, Baxter AE, Oldridge DA, Greenplate AR, Wu JE, Alanio C, D'Andrea K,
829 Kuthuru O, Dougherty J, Pattekar A, Kim J, Han N, Apostolidis SA, Huang AC, Vella LA,
830 Kuri-Cervantes L, Pampena MB, Betts MR, Wherry EJ, Meyer NJ, Cherry S, Bates P,
831 Rader DJ, Hensley SE. 2021. Seasonal human coronavirus antibodies are boosted upon

SARS-CoV-2 infection but not associated with protection. Cell 1–7.

54. Mateus J, Grifoni A, Tarke A, Sidney J, Ramirez SI, Dan JM, Burger ZC, Rawlings SA, Smith DM, Phillips E, Mallal S, Lammers M, Rubiro P, Quiambao L, Sutherland A, Yu ED, da Silva Antunes R, Greenbaum J, Frazier A, Markmann AJ, Premkumar L, de Silva A, Peters B, Crotty S, Sette A, Weiskopf D. 2020. Selective and cross-reactive SARS-CoV-2 T cell epitopes in unexposed humans. Science (80-) 370:89 LP – 94.

55. Lipsitch M, Grad YH, Sette A, Crotty S. 2020. Cross-reactive memory T cells and herd immunity to SARS-CoV-2. Nat Rev Immunol 20:709–713.

56. Altman DG. 1999. Practical statistics for medical research. Chapman & Hall/CRC, Boca Raton, Fla.

57. Hajian-Tilaki K. 2014. Sample size estimation in diagnostic test studies of biomedical informatics. J Biomed Inform 48:193–204.

58. Oguntuyo KY, Stevens CS, Hung C-T, Ikegame S, Acklin JA, Kowdle SS, Carmichael JC, Chiu H-P, Azarm KD, Haas GD, Amanat F, Klingler J, Baine I, Arinsburg S, Bandres JC, Siddiquey MN, Schilke RM, Woolard MD, Zhang H, Duty AJ, Kraus TA, Moran TM, Tortorella D, Lim JK, Gamarnik A V, Hioe CE, Zolla-Pazner S, Ivanov SS, Kamil JP, Krammer F, Lee B. 2020. Quantifying absolute neutralization titers against SARS-CoV-2 by a standardized virus neutralization assay allows for cross-cohort comparisons of COVID-19 sera. medRxiv Prepr Serv Heal Sci.

59. Wec AZ, Wrapp D, Herbert AS, Maurer DP, Haslwanter D, Sakharkar M, Jangra RK, Dieterle ME, Lilov A, Huang D, Tse L V., Johnson N V, Hsieh C-L, Wang N, Nett JH, Champney E, Burnina I, Brown M, Lin S, Sinclair M, Johnson C, Pudi S, Bortz R,

Wirchnianski AS, Laudermilch E, Florez C, Fels JM, O'Brien CM, Graham BS, Nemazee D, Burton DR, Baric RS, Voss JE, Chandran K, Dye JM, McLellan JS, Walker LM. 2020. Broad neutralization of SARS-related viruses by human monoclonal antibodies. Science eabc7424.

60. Schäfer A, Muecksch F, Lorenzi JCC, Leist SR, Cipolla M, Bournazos S, Schmidt F, Gazumyan A, Baric RS, Robbiani DF, Hatziioannou T, Ravetch J V, Bieniasz PD, Nussenzweig MC, Sheahan TP. 2020. Antibody potency, effector function and combinations in protection from SARS-CoV-2 infection in vivo. bioRxiv.

61. Valcourt EJ, Manguiat K, Robinson A, Chen JCY, Dimitrova K, Philipson C, Lamoureux L, McLachlan E, Schiffman Z, Drebot MA, Wood H. 2021. Evaluation of a commercially-available surrogate virus neutralization test for severe acute respiratory syndrome coronavirus-2 (SARS-CoV-2). Diagn Microbiol Infect Dis 99:115294.

62. Tseng YT, Wang SM, Huang KJ, I-Ru Lee A, Chiang CC, Wang CT. 2010. Self-assembly of severe acute respiratory syndrome coronavirus membrane protein. J Biol Chem 285:12862–12872.

63. Tasker S, Wight O'Rourke A, Suyundikov A, Jackson Booth P-G, Bart S, Krishnan V, Zhang J, Anderson KJ, Georges B, Roberts MS. 2021. Safety and Immunogenicity of a Novel Intranasal Influenza Vaccine (NasoVAX): A Phase 2 Randomized, Controlled Trial. Vaccines .

64. Sarzotti-Kelsoe M, Bailer RT, Turk E, Lin C, Bilska M, Greene KM, Gao H, Todd CA, Ozaki DA, Seaman MS, Mascola JR, Montefiori DC. 2014. Optimization and validation of the TZM-bl assay for standardized assessments of neutralizing antibodies against HIV-1.

876 J Immunol Methods 409:131–146.

877 65. Nguyen HT, Zhang S, Wang Q, Anang S, Wang J, Ding H, Kappes JC, Sodroski J. 2020.
878 Spike glycoprotein and host cell determinants of SARS-CoV-2 entry and cytopathic
879 effects. J Virol.

880 66. Weissman D, Alameh M-G, de Silva T, Collini P, Hornsby H, Brown R, LaBranche CC,
881 Edwards RJ, Sutherland L, Santra S, Mansouri K, Gobeil S, McDanal C, Pardi N,
882 Hengartner N, Lin PJC, Tam Y, Shaw PA, Lewis MG, Boesler C, Şahin U, Acharya P,
883 Haynes BF, Korber B, Montefiori DC. 2020. D614G Spike Mutation Increases SARS
884 CoV-2 Susceptibility to Neutralization. Cell Host Microbe.

885 67. Yurkovetskiy L, Wang X, Pascal KE, Tomkins-Tinch C, Nyalile TP, Wang Y, Baum A,
886 Diehl WE, Dauphin A, Carbone C, Veinotte K, Egri SB, Schaffner SF, Lemieux JE,
887 Munro JB, Rafique A, Barve A, Sabeti PC, Kyratsous CA, Dudkina N V, Shen K, Luban
888 J. 2020. Structural and Functional Analysis of the D614G SARS-CoV-2 Spike Protein
889 Variant. Cell 183:739-751.e8.

890 68. Korber B, Fischer WM, Gnanakaran S, Yoon H, Theiler J, Abfalterer W, Hengartner N,
891 Giorgi EE, Bhattacharya T, Foley B, Hastie KM, Parker MD, Partridge DG, Evans CM,
892 Freeman TM, de Silva TI, McDanal C, Perez LG, Tang H, Moon-Walker A, Whelan SP,
893 LaBranche CC, Saphire EO, Montefiori DC. 2020. Tracking Changes in SARS-CoV-2
894 Spike: Evidence that D614G Increases Infectivity of the COVID-19 Virus. Cell 182:812-
895 827.e19.

896 69. Centers for Disease Control and Prevention. 2021. SARS-CoV-2 Variant Classifications
897 and Definitions. Cdc.

70. Supasa P, Zhou D, Dejnirattisai W, Liu C, Mentzer AJ, Ginn HM, Zhao Y, Duyvesteyn HME, Nutalai R, Tuekprakhon A, Wang B, Paesen GC, Slon-Campos J, López-Camacho C, Hallis B, Coombes N, Bewley KR, Charlton S, Walter TS, Barnes E, Dunachie SJ, Skelly D, Lumley SF, Baker N, Shaik I, Humphries HE, Godwin K, Gent N, Sienkiewicz A, Dold C, Levin R, Dong T, Pollard AJ, Knight JC, Klenerman P, Crook D, Lambe T, Clutterbuck E, Bibi S, Flaxman A, Bittaye M, Belij-Rammerstorfer S, Gilbert S, Hall DR, Williams MA, Paterson NG, James W, Carroll MW, Fry EE, Mongkolsapaya J, Ren J, Stuart DI, Screaton GR. 2021. Reduced neutralization of SARS-CoV-2 B.1.1.7 variant by convalescent and vaccine sera. Cell 2201–2211.

71. Planas D, Bruel T, Grzelak L, Guivel-Benhassine F, Staropoli I, Porrot F, Planchais C, Buchrieser J, Rajah MM, Bishop E, Albert M, Donati F, Behillil S, Enouf V, Maquart M, Gonzalez M, Sèze J De, Péré H, Veyer D, Sève A, Simon-Lorière E, Fafi-Kremer S, Stefic K, Mouquet H, Hocqueloux L, Werf S van der, Prazuck T, Schwartz O. 2021. Sensitivity of infectious SARS-CoV-2 B.1.1.7 and B.1.351 variants to neutralizing antibodies. Nat Med 2021.02.12.430472.

72. Wang G-L, Wang Z-Y, Duan L-J, Meng Q-C, Jiang M-D, Cao J, Yao L, Zhu K-L, Cao W-C, Ma M-J. 2021. Susceptibility of Circulating SARS-CoV-2 Variants to Neutralization. N Engl J Med.

73. 2005. VALIDATION OF ANALYTICAL PROCEDURES: TEXT AND METHODOLOGY Q2(R1). Int Conf Harmon.

74. Stiles T, Grant V, Mawbey N, (Association). B. 2003. Good Clinical Laboratory Practice (GCLP): A Quality System for Laboratories that Undertake the Analyses of Samples from Clinical Trials. BARQA.

75. Sarzotti-Kelsoe M, Cox J, Cleland N, Denny T, Hural J, Needham L, Ozaki D, Rodriguez-Chavez IR, Stevens G, Stiles T, Tarragona-Fiol T, Simkins A. 2009. Evaluation and Recommendations on Good Clinical Laboratory Practice Guidelines for Phase I–III Clinical Trials. PLOS Med 6:e1000067.

76. Phillips N. 2021. The coronavirus is here to stay - here's what that means. Nature 590:382–384.

928 **Figures and Tables**

929 **Table 1. Demographic and exposure/symptom characteristics of study participants.**

Age	**n**	**%**
23-40	8	20
41-50	11	27.5
51-60	11	27.5
61-70	6	15
>70	4	10
Median	51.5	
Range	23-81	
Gender		
Female	16	40
Male	24	60
Exposures/symptoms		
Tested positive	8	20
Symptomatic contact of known positive	9	22.5
Symptomatic without confirmation	19	47.5
Asymptomatic contact of someone symptomatic	2	5
Asymptomatic, no exposures	2	5
Travel outside US since 12/1/19	7	17.5
Other		
Essential worker	6	15
Lives with children	14	35

930

931

932 **Table 2. SARS-CoV-2 neutralization assay platforms used in the study.**

	SARS-CoV-2/VeroE6	VSV-pseudo/Vero	LV-pseudo/293T	LV-pseudo/TZM-bl	HTS-LV-pseudo/293T	Surrogate Virus Neutralization Test (sVNT)
Lab	Baric	Corey	Montefiori	Montefiori	Huang/Jerome	Corey
Cell line	Vero E6	Vero	HEK293T	TZM-bl	HEK293T	None
ACE2 expression	Endogenous	Endogenous	Engineered	Engineered	Engineered	Recombinant
TMPRSS2 expression	No	No	No	Engineered	No	N/A
Virus shorthand	rSARS-CoV-2-nLuc	VSV-pseudo	LV-pseudo	LV-pseudo	HTS-LV-pseudo	N/A
Virus type	Live recombinant	VSV(G*ΔG-luciferase) pseudotyped	pCMV-ΔR8.2 lentiviral packaging with pHR'-CMV-Luc	pSG3ΔEnv lentiviral packaging	pHDM lentiviral packaging	N/A
SARS-CoV-2 strain/isolate	WA-CDC-WA1-A12/2020	Wuhan-Hu-1	Wuhan-Hu-1 (VRC7480) D614G	Wuhan-Hu-1 (VRC7480) D614G	Wuhan-Hu-1 D614G	Unknown
GenBank	MT020880.1	MN908947.3	MN908947.3	MN908947.3	MN908947.3	N/A
Amino acid 614	D	D	G	G	G	Unknown
Biosafety level	3	2	2	2	2	1

933

934 **Table 3. Calibration of SARS-CoV-2 neutralization assays using First WHO Standard for**

935 **anti-SARS-CoV-2 immunoglobulin**

First WHO International Standard for anti-SARS-CoV-2 immunoglobulin	VSV-pseudo/Vero		LV-pseudo/293T		HTS-LV-pseudo/293T	
	ND50	ND80	ND50	ND80	ND50	ND80
WHO Standard, GMT	1511	557	3047	567	4650	1396
Calibration factor (1000 IU/ml ÷ Standard GMT)	0.662	1.795	0.328	1.764	0.215	0.716
GMT neutralization titer among participants	309.7	102.8	177.9	41.96	271.7	86.3
Calibrated readout (IU/mL)	**205**	**184.5**	**58.4**	**74.0**	**58.4**	**61.8**

936

937

938

939 **Figure 1**. **SARS-CoV-2 neutralization and binding antibody concentration from COVID-19**
940 **convalescent patients.** (A) Concentration of IgG against SARS-CoV-2 spike, RBD,
941 nucleoprotein and tetanus toxoid measured in the Luminex binding antibody assay. (B)
942 Indexes reported by the Abbott Architect nucleoprotein IgG test. (C) ND50 and (D) ND80
943 neutralization titer measured using five SARS-CoV-2 neutralization assays for 40 plasma
944 samples from 40 participants. Each assay defined its own lower limit of detection (LOD) based
945 on the initial dilution: 50-fold for SARS-CoV-2/VeroE6, 20 for the LV and VSV pseudovirus
946 assays and 10 for the sVNT. Data below the LOD (open triangles) are plotted at LOD/2.
947 Number and percent of samples above the LOD are indicated above each plot. For each
948 assay, the box represents the extend of the inter-quartile range (IQR) with a line indicating the
949 median; whiskers extend to 1.5 times the IQR.

950

951 **Figure 2**. **Correlation among assay readouts measuring neutralization or antigen-**
952 **specific IgG concentration in plasma.** Heatmap color is determined by the Pearson's
953 correlation coefficient (*r,* annotations). Each panel includes either ND50 titers (A) or ND80
954 titers (B) and their correlation with sVNT % neutralization, SARS-CoV-2 specific IgG
955 concentration (Luminex bead-based assay), the quantitative index of the Abbott nucleoprotein
956 assay and tetanus toxoid-specific IgG concentration. ND50 and ND80 values below 50 were
957 truncated at 25.

958

959

Figure 1

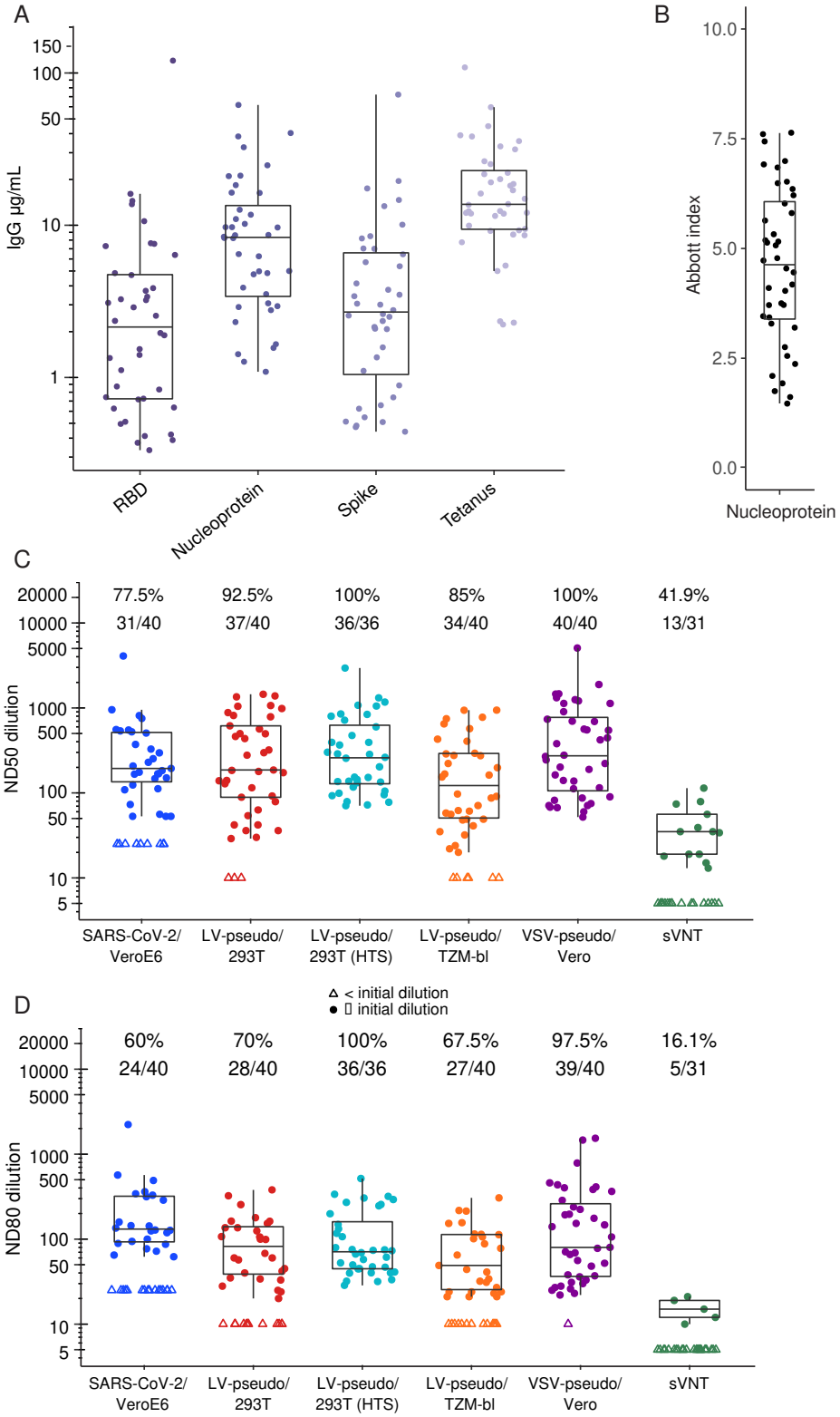

Figure 2

A

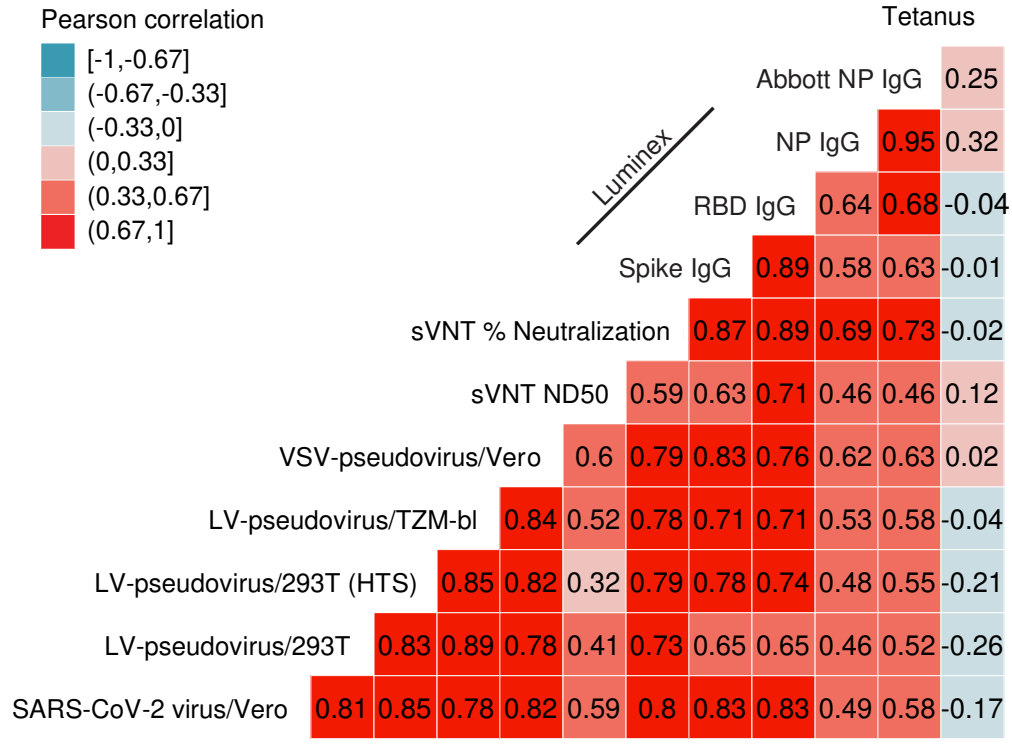

B

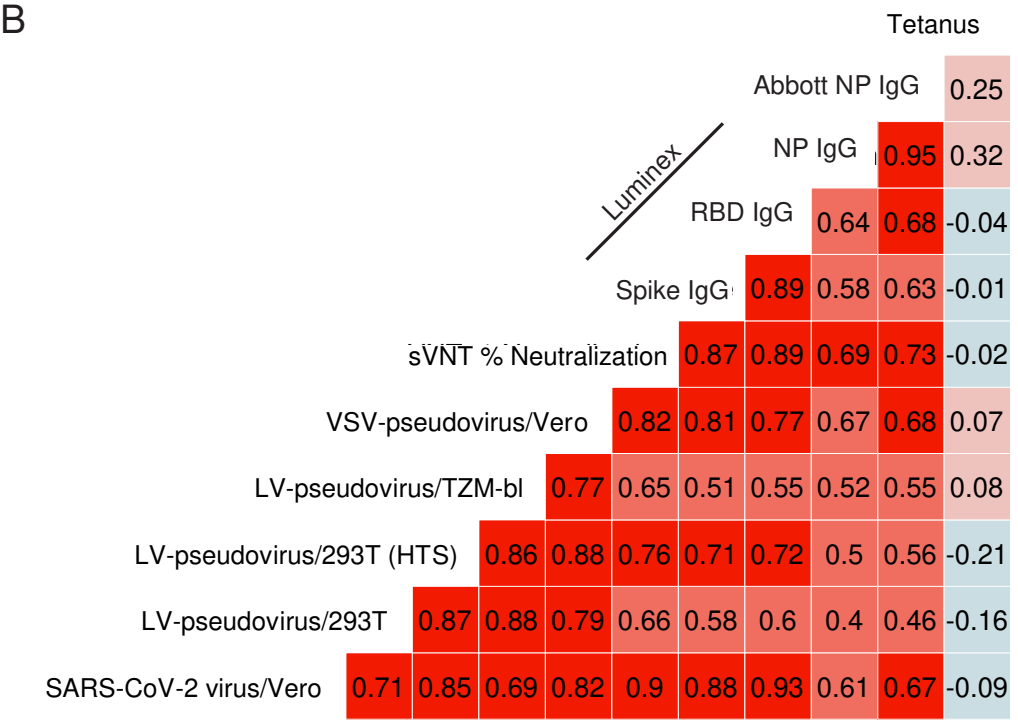

Evaluation of cell-based and surrogate SARS-CoV-2 neutralization assays

Running title (54 characters): Evaluation of SARS-CoV-2 neutralizing antibody assays

Anton M. Sholukh, Andrew Fiore-Gartland, Emily S. Ford, Maurine D. Miner, Yixuan J. Hou, Victor Tse, Haiying Zhu, Joyce Lu, Bhanupriya Madarampalli, Hannah Kaiser, Arnold Park, Florian A. Lempp, Russell Saint Germain, Emily Bossard, Jia Jin Kee, Kurt Diem, Andrew B. Stuart, Peter B. Rupert, Chance Brock, Matthew Buerger, Margaret K. Doll, April Kaur Randhawa, Leonidas Stamatatos, Roland K. Strong, Colleen McLaughlin, Meei-Li Huang, Keith R. Jerome, Ralph S. Baric, David Montefiori, and Lawrence Corey

Supplementary materials

Supplementary Methods

Protein antigens for the Luminex binding antibody assay. A recombinant form of a synthetic construct (SARS_CoV_2_ectoCSPP (1); GenBank: QJE37812.1) of the spike (S) glycoprotein from SARS-CoV-2 Wuhan-Hu-1 was produced in human HEK293 cells (FreeStyle™ 293-F Cells, ThermoFisher, Waltham, MA) using a lentivirus expression system (2) and purified by nickel affinity and size-exclusion chromatography. Purity and solution monodispersivity were confirmed by comparative reduced/non-reduced PAGE, analytical size-exclusion chromatography, and static/dynamic light scattering on Uncle (Unchained Labs, Pleasanton, CA) and showed uniform trimerization. The recombinant protein was modified by replacing the native leader sequence with a murine Igk leader, removing the polybasic S1/S2 cleavage site (RRAR to A), stabilized with a pair of proline mutations (2P), and incorporating a thrombin cleavage site, a T4 foldon trimerization domain, a hexa-histidine purification tag, and a C-terminal Avi-Tag (3). After purification, the protein was sterile filtered and aliquoted in DPBS, no calcium, no magnesium (ThermoFisher). Alternatively, spike protein was produced as described elsewhere (4). Both spike protein preparations were tested in a binding assay and no difference in recognition by serum and plasma samples from different convalescent subjects was found. Receptor binding domain (RBD) was produced in the same construct, swapping a tobacco etch virus (TEV) protease site (5) for the thrombin cleavage site. SARS-CoV-2 nucleoprotein was purchased from GenScript (Piscataway, NJ) and tetanus toxoid from Lonza (Basel, Switzerland).

In-house Luminex SARS-CoV-2 IgG binding antibody assay. Protein antigens were coupled to the Bio-Plex Pro Magnetic COOH beads in a ratio of 10 µg of antigen per 2.5 x 10^6 beads in a two-step carbodiimide reaction. First, beads were washed and resuspended in Activation Buffer (100 mM MES, pH 6) and then incubated with N-hydroxysulfosuccinimide (Sulfo-NHS, catalog number 24520; ThermoFisher) and 1-ethyl-3-[3-dimethlyaminopropyl]carbodiimide-HCl (EDC, catalog number 77149; ThermoFisher) also dissolved in Activation Buffer for 20 minutes on an end-over-end rotational mixer at room temperature protected from light. Activated beads were washed three times in Activation buffer. For coupling, antigen was mixed with activated beads and reaction was carried out for 2 h on a

rotational mixer at room temperature protected from light. Conjugated beads were washed three times with Wash buffer (PBS, 0.05% Tween-20, 1% BSA, 0.1% NaN_3) and finally resuspended in Wash buffer at 10^7 beads/ml. Beads were stored at 4 ºC for no longer than 30 days.

Antigen-specific IgG was measured using two replicate dilutions. Beads were blocked with phosphate buffered saline (PBS; Gibco) containing 5% Blotto (Bio-Rad) and 0.05% Tween-20 (Sigma) and incubated for 1 hour with serially diluted plasma samples. Next, beads were washed 3 times with 0.05% Tween-20 in PBS and incubated with anti-human IgG Fc-PE (catalog number 2048-09; Sothern Biotech). After incubation with secondary antibody, beads were washed and resuspended in PBS with 1% BSA and 0.05% Tween-20 and binding data were collected on Bio-Plex 200 instrument (Bio-Rad). Median Fluorescence Intensity (MFI) was measured for a minimum of 50 beads per region. Background was established by measuring the MFI of beads conjugated to antigens but incubated in Assay buffer. Background MFI values were subtracted from all readings. We also trialed unconjugated beads and beads conjugated to a decoy antigen with the same plasma samples used in testing and did not detect non-specific binding above the assay background described above.

An IgG standard curve run in duplicate was used to estimate IgG concentration. For that, anti-human IgG Fab-specific (Southern Biotech) was conjugated to MagPlex beads. IgG-coupled beads were blocked, washed and incubated with serially diluted human standard IgG (catalog number I4506; Sigma) for 1 h. Standard beads were washed and incubated with anti-human IgG Fc-PE and MFI was measured as described above. MFI readings and associated IgG concentrations were fitted to a four-parameter logistic curve (4PL) using the R packages *nCal* and *drc*. A standard curve for each experiment was used to obtain the effective concentrations of IgG in serum using the MFI measured with antigen-coated beads. Since plasma samples were also run as a dilution series we used the median of the estimated concentrations from the dilutions that yielded MFIs between 100 and 10,000. Plasma with all values above (below) this range were right (left) censored at the concentration of the minimum (maximum) MFI.

VSV-pseudovirus. The codon-optimized sequence of the SARS-CoV-2 spike protein (YP_009724390.1) with a truncation of the 19 C-terminal amino acids (D19) was cloned into a pcDNA3.1(+) vector (ThermoFisher) under control of the human CMV promoter to generate pcDNA3.1(+)-SARS-CoV-2-D19. The C-terminal truncation leads to a deletion of the ER-retention signal, localizing the spike protein to the cell surface, which enhances pseudovirus packaging (6). VSV(G*ΔG-luciferase) system was purchased from Kerafast (7, 8). Twenty-four hours prior infection with VSV(G*ΔG-luciferase), 293T cells were transfected with pcDNA-WuhanCoV-S-D19. Next day, supernatant was harvest, centrifuged for 5 min at 1,000xg, aliquoted and stored at -80 ºC. $TCID_{50}$ was measured by infecting Vero cells (catalog number CCL-81; ATCC) with serial 2-fold dilutions of the prepared pseudovirus.

LV-pseudovirus. An expression plasmid encoding codon-optimized full-length spike of the Wuhan-1 strain (VRC7480), was provided by Drs. Barney Graham and Kizzmekia Corbett at the Vaccine Research Center, National Institutes of Health (USA). The D614G mutation was introduced into VRC7480 by site-directed mutagenesis using the QuikChange Lightning Site-Directed Mutagenesis Kit from (catalog number 210518; Agilent Technologies). The mutation was confirmed by full-length spike gene sequencing. Pseudovirions were produced in HEK 293T/17 cells (catalog number CRL-11268; ATCC) by transfection using Fugene 6 (catalog number E2692; Promega). Pseudovirions for 293T/ACE2 infection were produced by co-transfection with a lentiviral backbone (pCMV-ΔR8.2) and firefly luciferase reporter gene (pHR'-CMV-Luc) (9). Pseudovirions for TZM-bl/ACE2/TMPRSS2 infection were produced by co-transfection with the Env-deficient lentiviral backbone pSG3ΔEnv (kindly provided by Drs Beatrice Hahn and Feng Gao). Culture supernatants from transfections were clarified of cells by low-speed centrifugation and filtration (0.45 µm filter) and stored in 1 ml aliquots at -80ºC.

Live SARS-CoV-2 neutralization assay. All the live virus experiments were performed under BSL-3 conditions at negative pressure, by operators in Tyvek suits wearing personal powered-air purifying respirators. Vero E6 cells were seeded at $2x10^4$ cells/well in a 96-well plate 24 h before the assay. Seventy five pfu of the recombinant SARS-CoV-2-nanoLuc virus (rSARS-CoV-2-nLuc) (10) were mixed

with Ab at 1:1 ratio and incubated at 37ºC for 1h. A 8-points, 3-fold dilution curve was generated for each sample with starting concentration at 1:50. Virus and Ab mix was added to each well and incubated at 37ºC + 5% CO_2 for 48h. Luciferase activities were measured by Nano-Glo Luciferase Assay System (Promega) following manufacturer protocol using SpectraMax M3 luminometer (Molecular Devices). Percent neutralization was calculated by the following equation: [1-(RLU with sample/ RLU with mock treatment)] x 100%.

VSV pseudovirus neutralization assay. Assay was carried out in BSL-2 laboratory. Vero cells (ATCC® CCL-81™) were seeded at $2x10^4$ cells/well in a black-walled 96-well plates 24 hours before the assay. A 7-point, 3-fold dilution curve was generated with starting sample dilution at 1:20 in a separate round-bottom 96-well plate. $3.8x10^2$ TCID50 of rVSV(G*ΔG-luciferase) pseudovirus with SARS-CoV-2-D19 spike protein (PsVSV-Luc-D19) was mixed with the plasma dilutions. Plasma-virus mixture was incubated at 37 ºC in 5% CO_2 for 30 minutes. After incubation, plasma-virus mixture was transferred onto the Vero cells. Cells were then incubated at 37 ºC, 5% CO_2 for 18-20 hours. Luciferase activity was measured by Bio-Glo Luciferase Assay System (catalog number G7940; Promega) following manufacturer protocol using 2030 VICTOR X3 multilabel reader (PerkinElmer). Percent virus neutralization was calculated by the following equation: [1-(luminescence of sample/ luminescence of cells+virus control)] x 100%.

LV-pseudovirus neutralization assays. Assays were carried out in BSL-2 laboratory. Neutralization of SARS-CoV-2 Spike-pseudotyped virus prepared with lentiviral vectors was performed by using infection in either HEK 293T cells expressing human ACE2 (293T/ACE2.MF) or TZM-bl cells expressing both ACE2 and TMPRSS2 (TZM-bl/ACE2/TMPRSS2 cells). Both cell lines kindly provided by Drs. Mike Farzan and Huihui Mu at Scripps). Cells were maintained in DMEM containing 10% FBS, 1% Pen Strep and 3 ug/ml puromycin.

293T/ACE2 cells pseudovirus assay. For the 293T/ACE2 assay, a pre-titrated dose of virus was incubated with serial 3-fold dilutions of test sample in duplicate in a total volume of 150 ul for 1 hr at

37°C in 96-well flat-bottom black/white culture plates. Freshly trypsinized cells (10,000 cells in 100 µl of growth medium) was added to each well. One set of control wells received cells + virus (virus control) and another set received cells only (background control). After 68-72 hours of incubation, 100 ul of cell lysate was transferred to a 96-well black/white plate (catalog number 6005060; Perkin-Elmer) for measurements of luminescence using the Promega Luciferase Assay System (catalog number E1501; Promega). Neutralization titers are the serum dilution at which RLUs were reduced by 50% and 80% compared to virus control wells after subtraction of background RLUs. MPI is the reduction in RLU at the lowest serum dilution tested.

ACE2/TMPRSS2 TZM-bl cells pseudovirus assay. For the TZM-bl/ACE2/TMPRSS2 assay, a pre-titrated dose of virus was incubated with serial 3-fold dilutions of test sample in duplicate in a total volume of 150 µl for 1 hr at 37°C in 96-well flat-bottom culture plates. Freshly trypsinized cells (10,000 cells in 100 ul of growth medium containing 75 µg/ml DEAE dextran) were added to each well. One set of control wells received cells + virus (virus control) and another set received cells only (background control). After 68-72 hours of incubation, 100 µl of cell lysate was transferred to a 96-well black solid plate (Costar) for measurements of luminescence using the BriteLite Luminescence Reporter Gene Assay System (PerkinElmer Life Sciences). Neutralization titers are the serum dilution at which relative luminescence units (RLU) were reduced by 50% and 80% compared to virus control wells after subtraction of background RLUs. Maximum percent inhibition (MPI) is the reduction in RLU at the lowest serum dilution tested.

SARS-CoV-2 Surrogate Virus Neutralization Test (sVNT). Assay was carried out in BSL-1 laboratory and was performed according to manufacturer (GenScript) protocol and recommendations as follows. Capture plate was incubated with plasma samples diluted 1:10, washed and probed with secondary antibody. Assay was developed via TMB (ThermoFisher) and OD at 450 nm was measured using SpectraMax M2 reader (Molecular Devices). Positive and negative controls were provided in the kit. Binding inhibition was determined via the following formula: Inhibition = (1 – (OD of sample / OD of Negative control)) × 100%. Percent binding inhibition was interpreted as a percent neutralization. In

order to determine ND50, plasma samples were serially diluted starting from 1:10 and assay was performed as described above.

Statistical Analysis and Visualization. Neutralization titers were defined as the plasma dilution that reduced relative luminescence units (RLU) by 50% or 80% relative to virus control wells (cells + virus only) after subtraction of background RLU in cells-only control wells. RLU was first transformed to neutralization using the formula neut = 1 – ([RLUsample – bkgd] / [RLUVO – bkgd]). The neutralization vs. dilution curve was then fit with a four-parameter logistic curve (4PL) model that was used to estimate the dilution at which there would be 50% or 80% neutralization. For samples with all dilutions having <50% neutralization the result was right censored at the highest concentration. Fifty and 80 percent neutralization titers (ND50 and ND80) were estimated using the nCal and drc packages in R. Patient demographic information (sex and age) was extracted from a RedEDCap survey database. Abbott assay results (including index value) were extracted from the laboratory information system (Sunquest Laboratory).

Correlations and group differences were estimated using parametric methods and testing (e.g. Pearson correlation and Student's t test). Log-transformed ND50 values and IgG concentrations were approximately normally distributed with few outliers and a low level of censoring, justifying use of these methods. Left censored values were given a value of half the level of detection, which corresponded to the first dilution for each neutralization assay.

References:

1. Wrapp D, Wang N, Corbett KS, Goldsmith JA, Hsieh CL, Abiona O, Graham BS, McLellan JS. 2020. Cryo-EM Structure of the 2019-nCoV Spike in the Prefusion Conformation. bioRxiv2020/06/09.

2. Bandaranayake AD, Correnti C, Ryu BY, Brault M, Strong RK, Rawlings DJ. 2011. Daedalus: a robust, turnkey platform for rapid production of decigram quantities of active recombinant proteins in human cell lines using novel lentiviral vectors. Nucleic Acids Res2011/09/14. 39:e143.

3. Ashraf SS, Benson RE, Payne ES, Halbleib CM, Gron H. 2004. A novel multi-affinity tag system to produce high levels of soluble and biotinylated proteins in Escherichia coli. Protein Expr Purif 33:238–245.

4. Seydoux E, Homad LJ, MacCamy AJ, Parks KR, Hurlburt NK, Jennewein MF, Akins NR, Stuart AB, Wan YH, Feng J, Whaley RE, Singh S, Boeckh M, Cohen KW, McElrath MJ, Englund JA, Chu HY, Pancera M, McGuire AT, Stamatatos L. 2020. Analysis of a SARS-CoV-2-Infected Individual Reveals Development of Potent Neutralizing Antibodies with Limited Somatic Mutation. Immunity 53:98-105.e5.

5. Cesaratto F, Lopez-Requena A, Burrone OR, Petris G. 2015. Engineered tobacco etch virus (TEV) protease active in the secretory pathway of mammalian cells. J Biotechnol 212:159–166.

6. Ou X, Liu Y, Lei X, Li P, Mi D, Ren L, Guo L, Guo R, Chen T, Hu J, Xiang Z, Mu Z, Chen X, Chen J, Hu K, Jin Q, Wang J, Qian Z. 2020. Characterization of spike glycoprotein of SARS-CoV-2 on virus entry and its immune cross-reactivity with SARS-CoV. Nat Commun 11:1620.

7. Whitt MA. 2010. Generation of VSV pseudotypes using recombinant DeltaG-VSV for studies on virus entry, identification of entry inhibitors, and immune responses to vaccines. J Virol Methods

169:365–374.

8. Zhao X, Howell KA, He S, Brannan JM, Wec AZ, Davidson E, Turner HL, Chiang C-I, Lei L, Fels JM, Vu H, Shulenin S, Turonis AN, Kuehne AI, Liu G, Ta M, Wang Y, Sundling C, Xiao Y, Spence JS, Doranz BJ, Holtsberg FW, Ward AB, Chandran K, Dye JM, Qiu X, Li Y, Aman MJ. 2017. Immunization-Elicited Broadly Protective Antibody Reveals Ebolavirus Fusion Loop as a Site of Vulnerability. Cell 169:891-904.e15.

9. Naldini L, Blömer U, Gage FH, Trono D, Verma IM. 1996. Efficient transfer, integration, and sustained long-term expression of the transgene in adult rat brains injected with a lentiviral vector. Proc Natl Acad Sci U S A 93:11382–11388.

10. Hou YJ, Okuda K, Edwards CE, Martinez DR, Asakura T, Dinnon KH, Kato T, Lee RE, Yount BL, Mascenik TM, Chen G, Olivier KN, Ghio A, Tse L V., Leist SR, Gralinski LE, Schäfer A, Dang H, Gilmore R, Nakano S, Sun L, Fulcher ML, Livraghi-Butrico A, Nicely NI, Cameron M, Cameron C, Kelvin DJ, de Silva A, Margolis DM, Markmann A, Bartelt L, Zumwalt R, Martinez FJ, Salvatore SP, Borczuk A, Tata PR, Sontake V, Kimple A, Jaspers I, O'Neal WK, Randell SH, Boucher RC, Baric RS. 2020. SARS-CoV-2 Reverse Genetics Reveals a Variable Infection Gradient in the Respiratory Tract. Cell 1–18.

Supplementary Figures and Tables

Supplementary Table 1. Symptoms reported by study participants.

Symptom	Yes	No	Missing	Percent reporting symptom
Fever	23	11	6	57.5
Chills	26	10	4	65
Fatigue	35	4	1	87.5
Myalgia	27	9	4	67.5
Sore throat	20	14	6	50
Cough	29	6	5	72.5
Rhinorrhea	24	10	6	60
Dyspnea	22	13	5	55
Wheezing	6	19	15	15
Chest pain	13	16	11	32.5
Other respiratory	8	17	15	20
Headache	27	8	5	67.5
Nausea	9	18	13	22.5
Abdominal pain	6	20	14	15
Diarrhea	14	16	10	35
Loss senses	26	8	6	65
Eye pain	7	19	14	17.5
Rash feet	2	21	17	5
Rash body	4	21	15	10

220

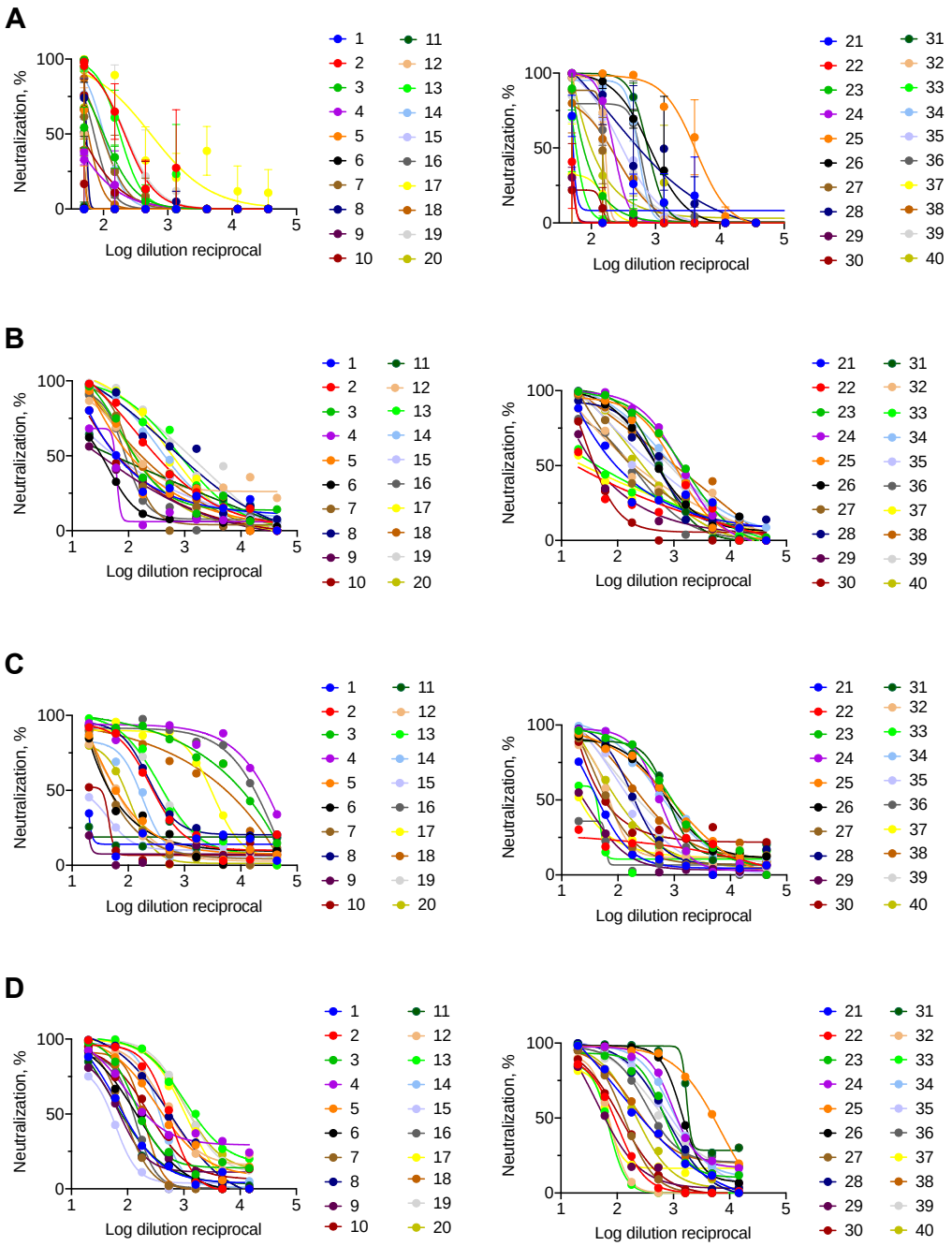

221 **Supplementary Figure 1. Neutralizing antibody assay.** (A) SARS-CoV-2-nLuc in Vero E6 cells. (B)

222 LV-pseudo in 293T/ACE2 cells. (C) LV-pseudo in TZM-bl/ACE2/TMPRSS2 cells. (D) PsVSV-Luc-D19

223 in Vero cells. Participant samples are as colored lines and circles numbered 1 – 40.

A

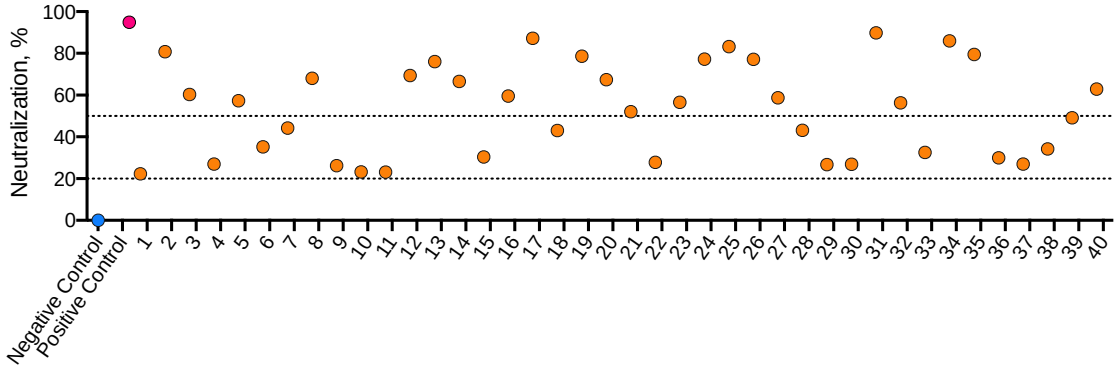

B

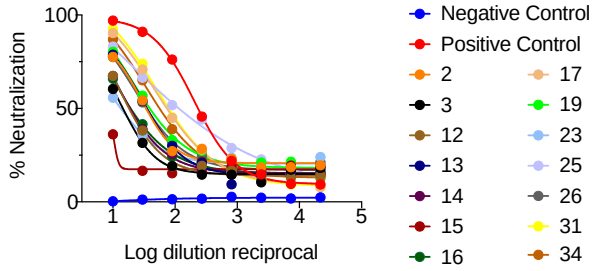

Supplementary Figure 2. Surrogate virus neutralization test from GenScript. A, samples tested in 1:10 dilution as per manufacturer protocol. Dotted lines show 50 and 20% neutralization, respectively. Twenty percent is suggested as positivity cutoff by the manufacturer. B, plasma samples were titrated 2-fold starting at 1:10 to impute ND50 titers.

234 **A**

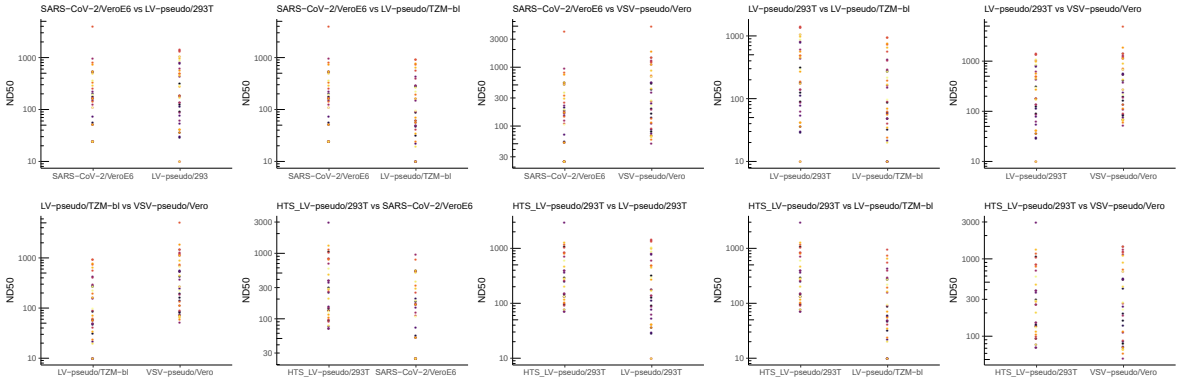

235

236

B

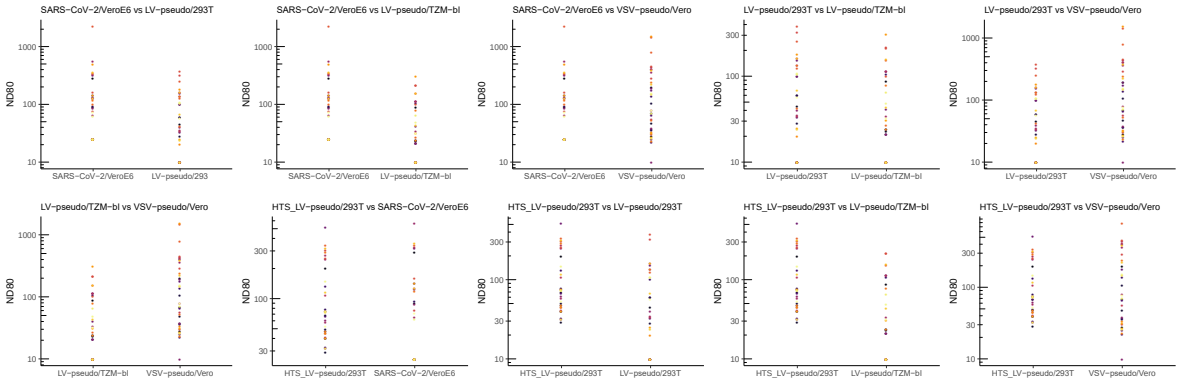

Supplementary Figure 3. Comparison of ND50 (A) and ND80 (B) titers measured in cell-based assays. Data used same as represented in Fig. 1 but replotted with lines connecting individual color-coded samples to illustrate the direction of ND50 and ND80 shift between assays.

Supplementary Table 2. GMT of ND50 and ND80 for each neutralization assay represented on Supplementary Figure 3, with fold-differences computed.

	Assay	GMT	95% CI LCL	95% CI UCL	fold-difference	Difference sign	Assay	GMT	95% CI LCL	95% CI UCL	N	p-value
ND50	SARS-CoV-2/VeroE6	141.3	93.7	213.0	12.8	>	sVNT	11.2	7.6	16.4	31	<0.001
	SARS-CoV-2/VeroE6	141.3	93.7	213.0	1.3	<	LV-pseudo/293T	177.9	112.0	282.7	40	0.112
	SARS-CoV-2/VeroE6	141.3	93.7	213.0	1.6	>	LV-pseudo/TZM-bl	89.9	57.0	141.9	40	0.003
	SARS-CoV-2/VeroE6	141.3	93.7	213.0	2.2	<	VSV-pseudo/Vero	309.7	211.3	454.0	40	<0.001
	sVNT	11.2	7.6	16.4	14.8	<	LV-pseudo/293T	177.9	112.0	282.7	31	<0.001
	sVNT	11.2	7.6	16.4	7.6	<	LV-pseudo/TZM-bl	89.9	57.0	141.9	31	<0.001
	sVNT	11.2	7.6	16.4	26.1	<	VSV-pseudo/Vero	309.7	211.3	454.0	31	<0.001
	LV-pseudo/293T	177.9	112.0	282.7	2.0	>	LV-pseudo/TZM-bl	89.9	57.0	141.9	40	<0.001
	LV-pseudo/293T	177.9	112.0	282.7	1.7	<	VSV-pseudo/Vero	309.7	211.3	454.0	40	0.002
	LV-pseudo/TZM-bl	89.9	57.0	141.9	3.4	<	VSV-pseudo/Vero	309.7	211.3	454.0	40	<0.001
	HTS_LV-pseudo/293T	271.7	266.8	643.4	1.92	>	SARS-CoV-2/VeroE6	141.3	93.7	213.0	36	<0.001
	HTS_LV-pseudo/293T	271.7	266.8	643.4	24.3	>	sVNT	11.2	7.6	16.4	31	<0.001
	HTS_LV-pseudo/293T	271.7	266.8	643.4	1.5	>	LV-pseudo/293T	177.9	112.0	282.7	36	<0.001
	HTS_LV-pseudo/293T	271.7	266.8	643.4	3	>	LV-pseudo/TZM-bl	89.9	57.0	141.9	36	<0.001
	HTS_LV-pseudo/293T	271.7	266.8	643.4	1.1	<	VSV-pseudo/Vero	309.7	211.3	454.0	36	0.856
ND80	SARS-CoV-2/VeroE6	79.3	54.8	114.8	13.0	>	sVNT	6.0	5.1	7.0	31	<0.001
	SARS-CoV-2/VeroE6	79.3	54.8	114.8	1.9	>	LV-pseudo/293T	42.0	28.8	61.1	40	<0.001
	SARS-CoV-2/VeroE6	79.3	54.8	114.8	2.4	>	LV-pseudo/TZM-bl	33.0	23.3	46.8	40	<0.001
	SARS-CoV-2/VeroE6	79.3	54.8	114.8	1.3	<	VSV-pseudo/Vero	102.8	69.0	153.2	40	0.027
	sVNT	6.0	5.1	7.0	6.8	<	LV-pseudo/293T	42.0	28.8	61.1	31	<0.001
	sVNT	6.0	5.1	7.0	5.5	<	LV-pseudo/TZM-bl	32.7	21.6	49.4	31	<0.001
	sVNT	6.0	5.1	7.0	16.6	<	VSV-pseudo/Vero	102.8	69.0	153.2	31	<0.001
	LV-pseudo/293T	42.0	28.8	61.1	1.3	>	LV-pseudo/TZM-bl	33.0	23.3	46.8	40	0.001
	LV-pseudo/293T	42.0	28.8	61.1	2.5	<	VSV-pseudo/Vero	102.8	69.0	153.2	40	<0.001
	LV-pseudo/TZM-bl	33.0	23.3	46.8	3.1	<	VSV-pseudo/Vero	102.8	69.0	153.2	40	<0.001
	HTS_LV-pseudo/293T	86.3	83.9	163.4	1.1	>	SARS-CoV-2/VeroE6	79.3	54.8	114.8	36	0.009
	HTS_LV-pseudo/293T	86.3	83.9	163.4	14.4	>	sVNT	6.0	5.1	7.0	31	<0.001
	HTS_LV-pseudo/293T	86.3	83.9	163.4	2.1	>	LV-pseudo/293T	42.0	28.8	61.1	36	<0.001
	HTS_LV-pseudo/293T	86.3	83.9	163.4	2.6	>	LV-pseudo/TZM-bl	33.0	23.3	46.8	36	<0.001
	HTS_LV-pseudo/293T	86.3	83.9	163.4	1.2	<	VSV-pseudo/Vero	102.8	69.0	153.2	36	0.759

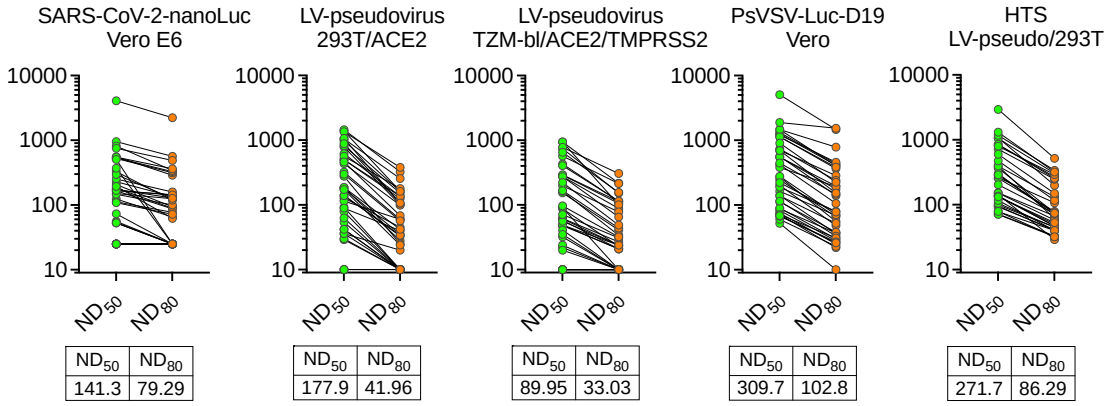

ND_{50}	ND_{80}
141.3	79.29

ND_{50}	ND_{80}
177.9	41.96

ND_{50}	ND_{80}
89.95	33.03

ND_{50}	ND_{80}
309.7	102.8

ND_{50}	ND_{80}
271.7	86.29

Supplementary Figure 4. Comparison of differences between geometric mean ND50 and ND80 titers for each neutralization assay. GMT ND50 and ND80 for the corresponding assay are shown underneath each graph. Each circle is a participant plasma sample, with lines connecting the same samples analyzed for the two neutralizing dilutions. Green circles are ND50 and orange circles are ND80 values.

254 **Supplementary Table 3. Fold change between ND50 and ND80 values.**

Assay	Mean ND fold change [95% CI]	P-value
SARS-CoV-2/Vero E6	1.954 [1.62, 2.29]	<0.0001
LV-pseudo/293T	4.573 [3.65, 5.5]	<0.0001
LV-pseudo/TZM-bl	4.478 [3.48, 5.48]	<0.0001
VSV-pseudo/Vero	2.967 [2.7, 3.24]	<0.0001
HTS_LV-pseudo/293T	3.303 [2.93, 3.68]	<0.0001

255

256

257

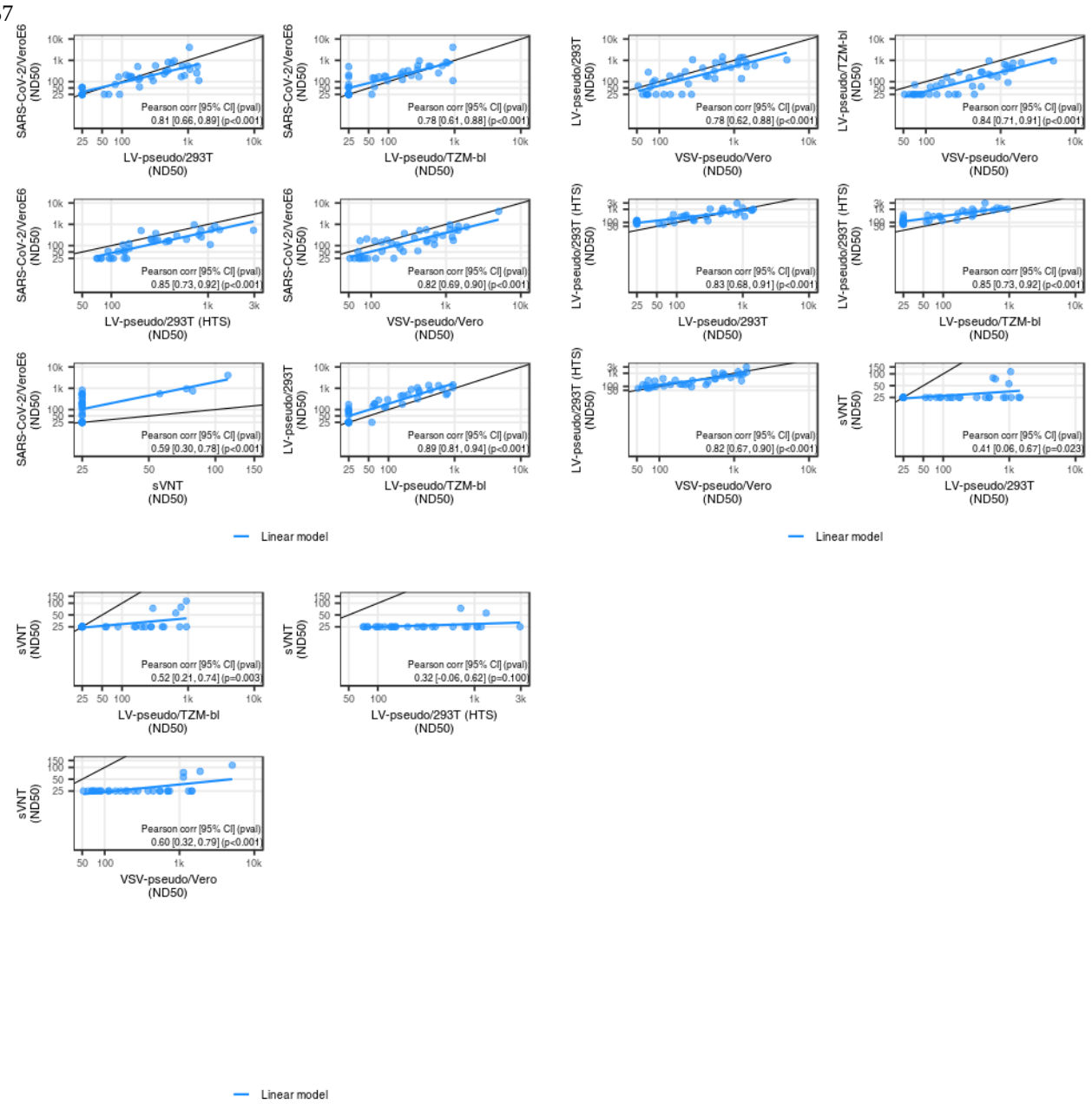

268

269 **Supplementary Figure 5. Pearson correlation model analysis of ND50 titers among**

270 **neutralization assays.**

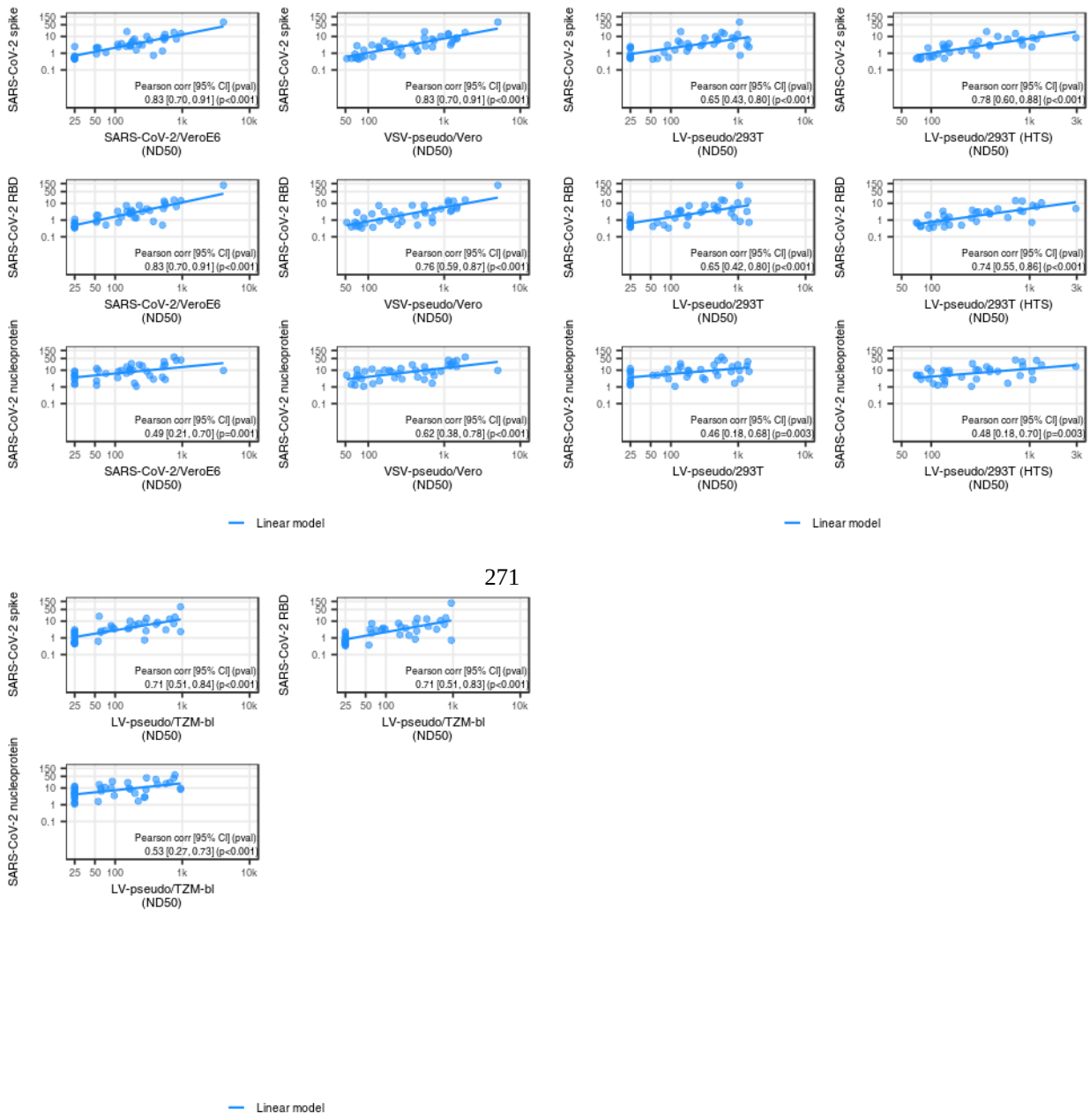

Supplementary Figure 6. Pearson correlation model analysis of ND50 titers vs SARS-CoV-2 specific IgG concentration in plasma samples.

Supplementary Table 4. Tests for association of SARS-CoV-2 antibody neutralization and binding with age of participants.

Assay	Measure	N	Age rho[1] (p-value)
SARS-CoV-2/VeroE6	ND50	40	0.28 (0.0751)
VSV-pseudo/Vero	ND50	40	0.30 (0.0602)
LV-pseudo/293T	ND50	40	0.24 (0.1288)
LV-pseudo/TZM-bl	ND50	40	0.27 (0.0885)
sVNT neutralization	ND50	31	0.43 (0.0160)
SARS-CoV-2/VeroE6	ND80	40	0.51 (0.0007)
VSV-pseudo/Vero	ND80	40	0.32 (0.0466)
LV-pseudo/293T	ND80	40	0.32 (0.0444)
LV-pseudo/TZM-bl	ND80	40	0.29 (0.0738)
sVNT neutralization	ND80	31	0.50 (0.0038)
sVNT neutralization (1:10 dilution)	%	40	0.40 (0.0106)
Abbott nucleoprotein	index	40	0.45 (0.0034)
SARS-CoV-2 spike-specific IgG	µg/mL	40	0.37 (0.0197)
SARS-CoV-2 RBD-specific IgG	µg/mL	40	0.45 (0.0035)
SARS-CoV-2 nucleoprotein-specific IgG	µg/mL	40	0.39 (0.0126)
Tetanus toxoid-specific IgG	µg/mL	40	-0.14 (0.3853)

[1]Spearman's rank correlation coefficient
[2]fold-difference indicates the geometric mean value in females/males, Student's *t* test p-value

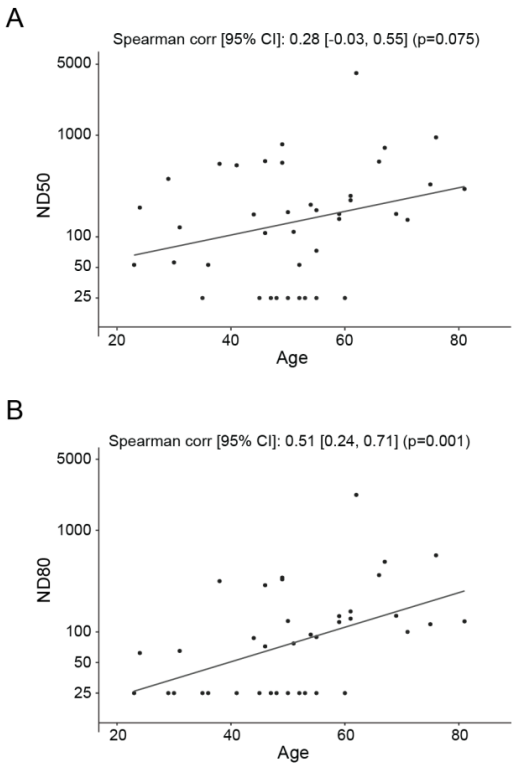

Supplementary Figure 7. **Correlation analysis of plasma neutralizing potency and age of participants.** (A) ND50 versus age. (B) ND80 versus age.

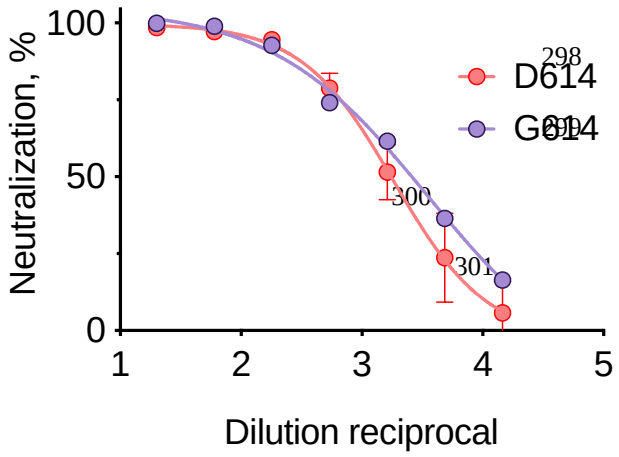

	G614	D614
ND50	2584	1741
ND80	465	516

Supplementary Figure 8. **Comparison of neutralization of VSV-pseudovirus bearing D614 and G614 mutations by the WHO standard.** Red, VSV-pseudoviruses with D614; Purple, VSV-pseudoviruses with G614.